AD_____

Award Number: DAMD17-98-1-8157

TITLE: A Low-Cost, High Quality MRI Breast Scanner Using Prepolarization

PRINCIPAL INVESTIGATOR: Albert Macovski, Ph.D.

CONTRACTING ORGANIZATION: Stanford University
Stanford, California 94305 -3027

REPORT DATE: October 1999

TYPE OF REPORT: Annual

PREPARED FOR: U.S. Army Medical Research and Materiel Command
Fort Detrick, Maryland 21702-5012

DISTRIBUTION STATEMENT: Approved for public release
distribution unlimited

The views, opinions and/or findings contained in this report are those of the author(s) and should not be construed as an official Department of the Army position, policy or decision unless so designated by other documentation.

DTIC QUALITY INSPECTED 4

20010108 121

REPORT DOCUMENTATION PAGE

Form Approved
OMB No. 074-0188

Public reporting burden for this collection of information is estimated to average 1 hour per response, including the time for reviewing instructions, searching existing data sources, gathering and maintaining the data needed, and completing and reviewing this collection of information. Send comments regarding this burden estimate or any other aspect of this collection of information, including suggestions for reducing this burden to Washington Headquarters Services, Directorate for Information Operations and Reports, 1215 Jefferson Davis Highway, Suite 1204, Arlington, VA 22202-4302, and to the Office of Management and Budget, Paperwork Reduction Project (0704-0188), Washington, DC 20503

1. AGENCY USE ONLY (Leave blank)	2. REPORT DATE	3. REPORT TYPE AND DATES COVERED
	October 1999	Annual (01 Oct 98 - 30 Sep 99)

4. TITLE AND SUBTITLE
A Low-Cost, High Quality MRI Breast Scanner Using Prepolarization

5. FUNDING NUMBERS
DAMD17-98-1-8157

6. AUTHOR(S)
Albert Macovski, Ph.D.

7. PERFORMING ORGANIZATION NAME(S) AND ADDRESS(ES)
Stanford University
Stanford, California 94305 -3027

e-mail:
macovski@Isl.stanford.edu

8. PERFORMING ORGANIZATION REPORT NUMBER

9. SPONSORING / MONITORING AGENCY NAME(S) AND ADDRESS(ES)
U.S. Army Medical Research and Materiel Command
Fort Detrick, Maryland 21702-5012

10. SPONSORING / MONITORING AGENCY REPORT NUMBER

11. SUPPLEMENTARY NOTES

12a. DISTRIBUTION / AVAILABILITY STATEMENT
Approved for public release
distribution unlimited

12b. DISTRIBUTION CODE

13. ABSTRACT ***(Maximum 200 Words)***

Magnetic Resonance Imaging (MRI) has been shown to be more sensitive and equally specific when compared to x-ray mammography for detecting breast cancer. MRI is non-invasive, completely non-toxic, and requires no uncomfortable breast compression. But an x-ray mammogram costs about $100 whereas an MRI study costs about $1,500. The exam cost is related to the scanner's manufacturing cost (≈ $400,000), and sale price ($1-3M). X-ray mammography units cost about one tenth of an MRI scanner.

Our objective is to tailor a new concept in MRI called Prepolarized MRI (PMRI) for low-cost MR mammography. PMRI substitutes two inexpensive pulsed magnets for the expensive superconducting magnet. We believe that a high-quality MRI breast scanner using prepolarization could be manufactured for less than $50,000. This project could potentially make MRI as affordable as x-ray mammography. In earlier work supported by DARPA and the Whitaker Foundation, we developed a Prepolarized MRI extremity scanner for $45,000. Breast imaging presents several unique engineering challenges, including tailored magnet design and extremely sensitive receiver coil design.

14. SUBJECT TERMS	15. NUMBER OF PAGES
Breast Cancer	30
	16. PRICE CODE

17. SECURITY CLASSIFICATION OF REPORT	18. SECURITY CLASSIFICATION OF THIS PAGE	19. SECURITY CLASSIFICATION OF ABSTRACT	20. LIMITATION OF ABSTRACT
Unclassified	Unclassified	Unclassified	Unlimited

NSN 7540-01-280-5500

Standard Form 298 (Rev. 2-89)
Prescribed by ANSI Std. Z39-18
298-102

FOREWORD

Opinions, interpretations, conclusions and recommendations are those of the author and are not necessarily endorsed by the U.S. Army.

_✓_ Where copyrighted material is quoted, permission has been obtained to use such material.

_✓_ Where material from documents designated for limited distribution is quoted, permission has been obtained to use the material.

_✓_ Citations of commercial organizations and trade names in this report do not constitute an official Department of Army endorsement or approval of the products or services of these organizations.

Does NOT Apply In conducting research using animals, the investigator(s) adhered to the "Guide for the Care and Use of Laboratory Animals," prepared by the Committee on Care and use of Laboratory Animals of the Institute of Laboratory Resources, national Research Council (NIH Publication No. 86-23, Revised 1985).

_✓_ For the protection of human subjects, the investigator(s) adhered to policies of applicable Federal Law 45 CFR 46.

Does NOT Apply In conducting research utilizing recombinant DNA technology, the investigator(s) adhered to current guidelines promulgated by the National Institutes of Health.

Does NOT Apply In the conduct of research utilizing recombinant DNA, the investigator(s) adhered to the NIH Guidelines for Research Involving Recombinant DNA Molecules.

Does Not Apply In the conduct of research involving hazardous organisms, the investigator(s) adhered to the CDC-NIH Guide for Biosafety in Microbiological and Biomedical Laboratories.

Albert Macovski 09 29 1999

PI - Signature Date

4 Table of Contents

1. Front Cover 1
2. Standard Form 298 Documentation Page 2
3. Foreword 3
4. Table of Contents 4
5. Introduction 5
6. Body 5
7. Key Research Accomplishments 13
8. Reportable Outcomes 15
9. Conclusions 16
10. References 16
11. Appendices 19

5 Introduction

The objective of this research is to develop a new concept in magnetic resonance imaging called Prepolarized MRI (PMRI) for low-cost MR mammography. Although MRI has been shown to be useful for the noninvasive diagnosis of breast cancer, x-ray mammography remains dominant because an MRI study costs more than ten times as much as an x-ray mammogram. We believe that a high-quality MRI breast scanner using prepolarization could be manufactured for less than $50,000, which is about 10% of the manufacturing cost of a conventional MRI scanner. Breast imaging presents several unique technical challenges for the PMRI concept. First, we must accommodate the patient's torso into the magnet configuration. Second, since breast tissue is relatively nonconductive we will need to use extremely sensitive receiver coils to obtain optimal image quality. Finally, we will need to develop PMRI pulse sequences that suppress fat and provide high quality 3D images.

6 Body

6.1 Design of the Biplanar Readout Magnet

The challenge here is to design the coils radii, z locations and currents to create an extremely homogeneous (10 ppm over a 15 cm radius volume) magnetic field of about 70 mT around the patient's breast. The problem is complicated by several constraints: we must minimize the cost of the magnet; the power must be manageable (less than about 20 kW, say); the magnet should be as open as possible for patient and physician access; and there are very significant practical concerns with both machining tolerances and temperature variations.

Our progress on the biplanar readout magnet this year has been excellent. The key fabrication challenges are (a) software for coil layout, (b) framing and cooling, and (c) the coil fabrication process, especially in dealing with normal machining errors. Each of these problems and our solutions are discussed below.

Magnet Design: Coil Layout We have studied both classic and modern magnet design techniques. In the classical magnet design techniques of Garrett and others [1, 2, 3, 4, 5, 6, 7, 8] the magnet coil radii, z locations, and currents were precisely chosen to make the field as flat as possible at the origin. The classic approach is effective for designing magnets with coils constrained to lie on a cylinder or on a sphere, but is too inflexible to handle the arbitrary coil arrangements necessary for cardiac MRI.

Whereas classic techniques used nonlinear optimization to find the coil radii, position and currents, more recent approaches enumerate *every* feasible coil location and radii. The length and diameter of the magnet are implicitly constrained by the layout of the feasible coils. All achievable fields, $\mathbf{b}$, can then be expressed as a linear function of the currents in the feasible coils:

$$\mathbf{b} = A\mathbf{i},$$

where $\mathbf{i}$ is the (vector) current in the N feasible coils, $\mathbf{b}$ is the B_z field at M target points, and A_{mn} is the field contribution from a unit current in the nth coil at the mth target point. Formulas for A_{mn} using elliptic integrals are well known [9]. This approach obviates nonlinear

optimization of the radii and z locations of the coils. But it poses a serious pruning problem since a buildable magnet can have no more than a dozen coils, and we require several hundred feasible coils for adequate position resolution. The number of target points is typically about twenty.

Several approaches have been proposed to select a small number of coils to satisfy the homogeneity constraints. Direct inversion approaches (using either the inverse or pseudoinverse of A) are ill-posed since the matrix A is extremely poorly conditioned. So these approaches produce impractical magnets with hundreds of non-zero currents that often fluctuate wildly [10, 11, 12, 13]. Other techniques have been developed to optimize passively shielded magnet [14, 15, 16, 17, 18, 19] and actively shielded magnets [20, 21, 13, 22, 23]. But these cannot easily handle arbitrarily shaped homogeneous field of view (FOVs) and arbitrary coil placement.

We recently developed an algorithm with significant advantages over approaches in the literature. For a series-wound magnet, the length of conductor is proportional to conductor cost (relevant to superconductor magnets) and magnet power (relevant to resistive magnets). Hence our algorithm minimizes the length of the wire subject to field homogeneity inequality constraints [24, 25, 26]. The optimization problem can be expressed as

$$\begin{aligned} \text{Minimize} \quad &: \quad \sum_{n}^{N} r_n |\mathbf{i}_n| \\ \text{Subject to} \quad &: \quad |A\mathbf{i} - B_0| \leq B_0 \epsilon, \end{aligned}$$

where ϵ is the fractional peak inhomogeneity, typically about 10^{-6}, or 1 ppm, and r_n is the radius of the nth coil. This is a classic optimization problem called an "L1-norm problem," and can be solved very efficiently using Linear Programming (LP) [27]. The algorithm automatically chooses the minimum number of nonzero currents necessary. It is also simple to incorporate shielding constraints and maximum current constraints. The homogeneous FOV can be any shape and the feasible coils can be at any position. Using MATLAB's standard lp() function, we can handle up to 200 feasible coil elements to compute a 1 ppm magnet in less than 20 seconds on our SUN Ultra 2. The algorithm is illustrated in Fig. 1. We usually start with a 2 cm grid and finish three iterations later with resolution of 0.1 mm. Instead of ideal filamentary loops, we use the field formula for thick loops [28, 29] during secondary calculations.

We applied the L1 norm software to layout a homogeneous biplanar magnet for our low-cost Prepolarized MRI scanner for breast imaging. The patient constraints illustrate the flexibility of the minimum-power magnet design algorithm. We chose a biplanar magnet to maximize openess. To minimize magnet power we used an asymmetric homogeneous volume (marked by diameter spherical volume, or DSV), as seen in Figure 2. The asymmetric design, shown in Fig. 3 is open, and requires 33% less power than a symmetric biplanar design. Due to budget restrictions (our original $100,000 budget was cut to just $70,000), we could not afford to put this magnet out for a construction bid in Year 1. However, this is our preferred magnet configuration for mammography. We are also considering other configurations, including a whole body cylindrical magnet that could be useful. The principal advantage of cylindrical systems is that we can use some of the existing magnets paid for under our other grants. Below we show the blueprints for our first body-sized (12-inch bore) homogeneous imaging magnet.

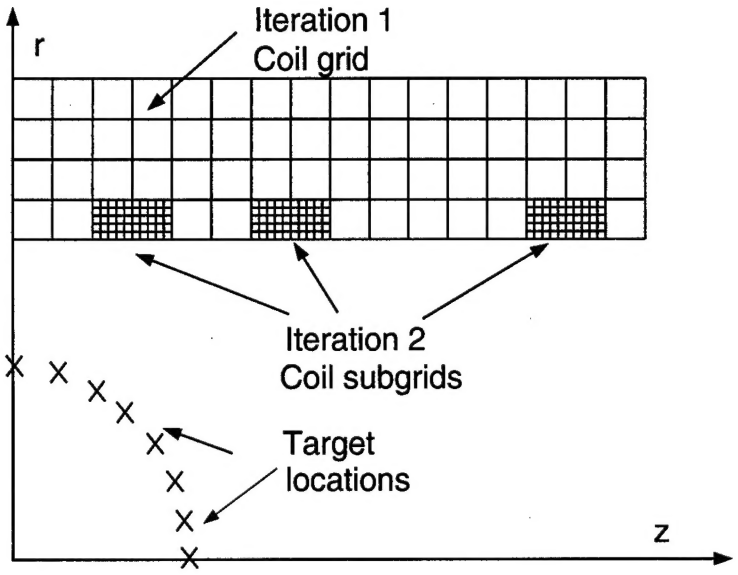

Figure 1: Our magnet design procedure uses Linear Programming to select a few non-zero current loops from the feasible coil grid. On subsequent iterations we focus a higher resolution grid of feasible coils over the selected coils. Three iterations is typically adequate to design a 1 ppm homogeneity magnet in less than a minute.

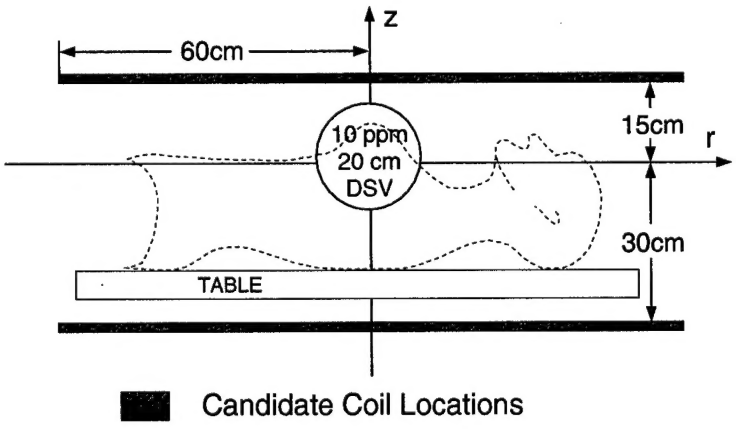

Figure 2: Feasible coil locations for the breast PMRI scanner shown in Fig. 3. The DSV is asymmetric.

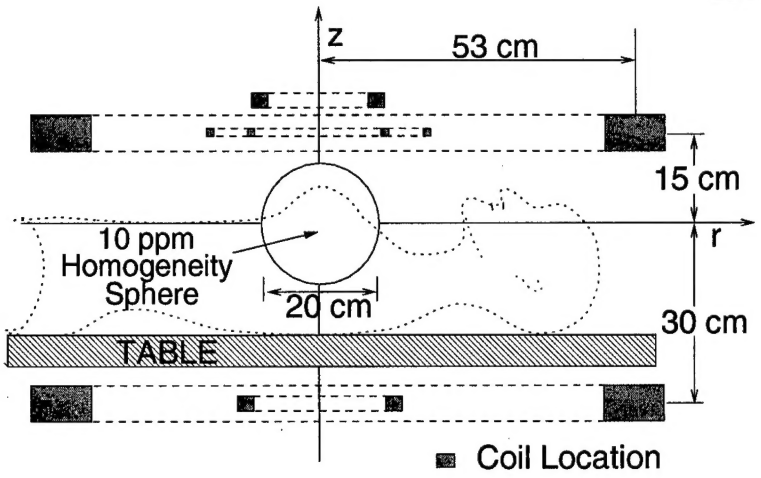

Figure 3: Mammography magnet picked from Fig.2. This reduces power by 33% without compromising access.

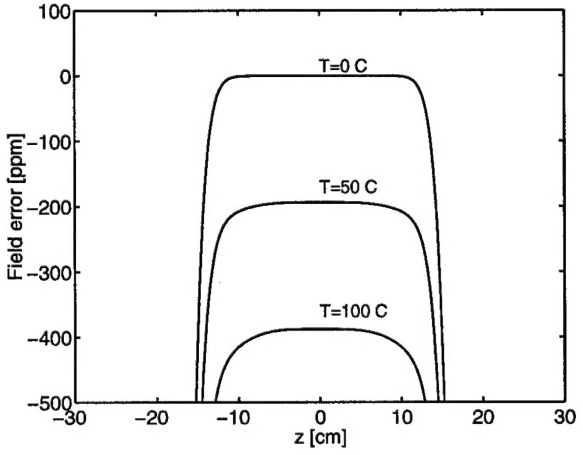

Figure 4: Simulated field plots for various temperatures. A 50°C temperature rise changes the center frequency of a homogeneous magnet by 400 Hz due to thermal expansion of the coils. Hence we use water cooling to stabilize the magnet temperature.

Magnet Design: Framing and Cooling Our first homogeneous electromagnet cost $17,000 and had no water cooling. The temperature increased at about 5 C/min, which made the field too unstable for MRI. As the coil temperature increases, the coils expand minutely, which causes the magnetic field to drop. The magnetic field is extremely sensitive to small expansions. Figure 4 shows the effect of temperature. A 50°C temperature rise causes a 200 ppm change in the center frequency (400 Hz at 2 MHz center frequency).

To stabilize the magnet temperature we spent a significant fraction of the last year devising new methods for water cooling the magnet. The three most popular methods of water cooling are [30] (1) wire wound coils with surface cooling through an enamel insulator; (2) hollow copper wire with water cooling through the center of the wire; and (3) tape coils surface cooled on their edges or or faces. The first method has very simple hydraulics and is inexpensive,

but it can cool only modest current densities due to the substantial thermal gradient across the wire enamel insulation layer. The second method has no thermal insulator between the water coolant and the copper so it can handle much higher current densities. However, the hydraulic design greatly complicates the magnet layout. The third method has insulation only between layers so it can cool a significant current density and the construction method is quite inexpensive. Hence we have adopted the edge cooled tape construction method.

The tape can be purchased with the precise thickness needed for the particular coil, with tolerance of 4 mils (a mil is a thousandths of an inch; it is the standard measure for the U.S. precision machinining industry). The copper foil layers are insulated with 1/4 mil mylar. We use 4 mil and 8 mil copper for the coils.

To test this cooling method, we designed a 12-inch bore homogeneous using six coils with 400 A/cm^2 current density. The magnet is now being constructed by Alpha Magnetics of Hayward CA under our direction. We are using a 1 mil thick Kapton insulation layer between the copper diffuser plate and the copper foil. The diffuser minimizes the temperature gradient across the insulator. There are three heat transfer mechanisms: convection between the water and its pipe, conduction across the insulation barrier, and conduction across the copper tape. We wrote several software simulators to predict each of the temperature gradients due to these mechanisms. The software allows for variations in the water flow rate, and the diameter and length of copper refrigerator tubing. We optimized all of these parameters to minimize the variation in temperature across the coils.

The final cooling design is shown in the Alpha Magnetics blueprint, included in the Appendix. Note that we used two separate cooling paths to increase flow rates. Our magnet dissipates a total of 3.6 kW at a 3 MHz center frequency. We recently found 1 mil thick Kapton is an ideal electrical insulator. We expect about 5 mils of epoxy in the insulation as well. We chose quarter-inch refrigerator tubing which gave adequate flow rate at 40 psig. With our optimized cooling design, we computed all the temperature gradients and found that our expected temperature variations between the coils is less than 10 C. Our magnet simulations indicate that the field temporal and spatial homogeneity will be adequate with this level of stability.

Robust Magnet Fabrication On our first readout magnet design, we found that most dimensions of the coils, including the axial and inner radii of the coils, were machinable to within 4 mils tolerance. But there is one dimension, namely the outer radius of the coils, that has a tolerance of 50 mils. This is due to the accumulation of small winding errors and slight bulges in the wire and insulation as it is laid down. Our simulations indicated that this error level in the outer radius can cause severe image artifacts.

The classic approaches to deal with these machining tolerances is to allow for some method to "shim" the magnet, usually electrically. Virtually all MRI scanners today have active shims, which are extra coil loops with individual power supplies designed to remove field inhomogeneity due to magnet imperfections and patient susceptibility varations. Other magnets rely on passive shimming, which means the placement of ferrous object (usually bricks or pole pieces) to reduce variations in the magnetic field.

These approaches are not extremely expensive but they do not work well with the PMRI concept. Passive shimming pieces could pose hysteresis problems after the pulsing of the polarizing magnet. And active shimming methods require a significant number of ultra-stable

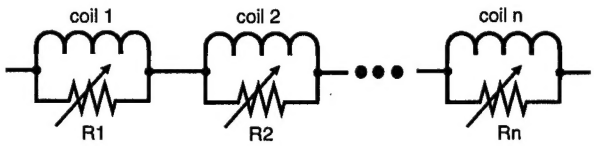

Figure 5: Variable resistors can adjust the current in each coil to regain homogeneity lost due to normal machining variations.

(albeit low power) current supplies. For PMRI we needed a less expensive and more reliable method.

For our first readout magnet, we relied on mechanical shimming of our first readout magnet [31]. This approach requires that each coil be axially adjustable, which was extremely expensive. Recently we have tested a passive electrical shimming technique [32] shown in Fig. 5. Adjustable resistors connected in parallel across each coil shunt a small fraction of the current out of the coil. Our simulations indicate that this method can compensate for normal machining variations ($\approx$ 0.1 mm) in the axial position. The simulations indicate, however, that this technique is inadequate to fully compensate for the much larger and more troublesome radial variations.

Hence, for our latest 12-inch readout magnet design we have pushed this concept even further by using three resistors per coil to compensate for variations in both radius and axial position. We include a blueprint in the Appendix that shows the overall layout for the homogeneous magnet. Each of the six coils is broken in two pieces to allow for separate shimming of radial variations. This increases the cost of the magnet only slightly since the shim currents are less than 1 % of the main coil current. We have determined through extensive and redundant simulation that this new method will allow us to shim out variations of even 100 mils in the outer radius using very inexpensive resistors. We estimate that the shim resistors will need to dissipate about 20 W.

We have exploited the L1 norm magnet design, edge water cooling, and resistive shimming to design our first human sized readout magnet this year: a 12-inch bore magnet with 3 MHz center frequency. The magnet will be completed by the magnet design company Alpha Magnetics within the next three weeks. They bid just $6720 to construct this system and another $11,000 for an integral polarizing coil. Their bid was quite encouraging since it proves that the two principal magnets for a *patient-sized* PMRI system can indeed be constructed for less than $20,000.

6.2 Receiver Subsystem Progress

The key challenges of the receiver system for breast PMRI involve achieving the highest SNR and imaging speed limited only by fundamental physical constraints rather than by hardware limits. Not only must the preamplifier and receiver coil be very low noise, but the radio frequency interactions with the other PMRI components such as the polarizing coil must be minimized. Work has progressed on the design of the preamplifier topologies, new receiver coil cryostats, and shielding methods to limit RF losses from the polarizing coil.

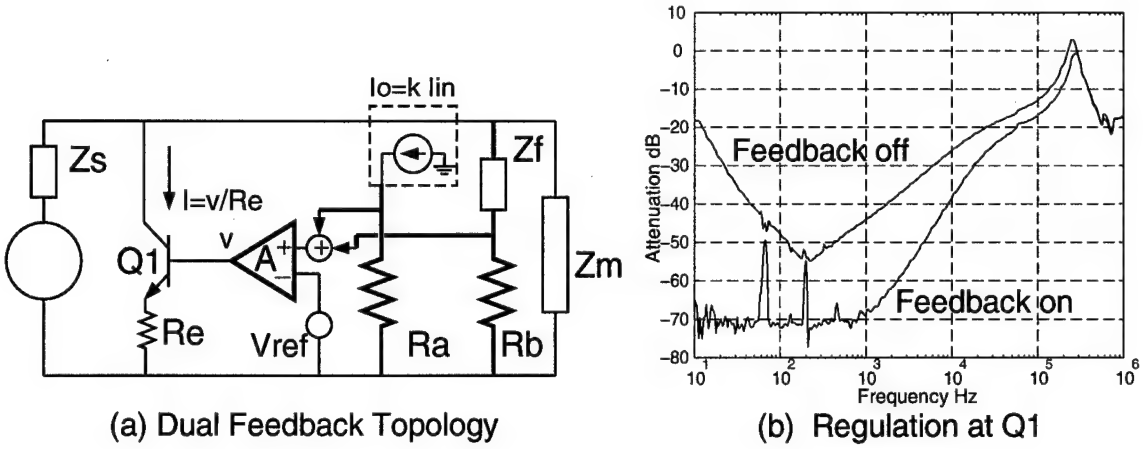

Figure 6: Field Stabilization (a) Dual feedback topology allows the effective output impedance to be adjusted for the current source. (b) Regulation for injected error current approaches 70 dB

Shielding Since the prepolarizing coil is intended to boost the SNR of a low field system, any noise introduced by this coil must be eliminated in the PMRI receiver. Our testing indicated that at RF frequencies, a closely wound prepolarizing coil had RF losses significantly higher than those from the patient. This would mean that PMRI would have significantly worse SNR than conventional MRI— a potential show-stopper.

Fortunately we found that we could prevent this extra noise source from entering the receiver by shielding the RF coil from the polarizing coil. We did this by inserting a conducting cylinder in between them. The RF shield between the receiver coil and polarizing essentially removes this extra noise source. The only tradeoff is a slight attenuation of the RF amplitude inside the RF coil, which will reduce our imaging speed.

To quantify this loss of imaging speed, we created several computer simulation models to predict shield behavior on the receiver SNR. We have found that for a coil radius of c and a shield radius of b, the RF field inside the coil is shielded by the factor $(1 - b^2/c^2)$. Hence, with a shield diameter double the receiver diameter, the receiver coil will still retain 75% of its inherent sensitivity. This was quite reassuring.

The design of the RF shield is quite simple. It must appear open at low frequencies (to prevent eddy currents) and as a short at higher frequencies. We have tested a simple copper cylinder with a axial slit down its length, joined by many capacitors. We are also looking at more distributed capacitor patterns to optimize shield behaviour.

In summary, a potentially fatal noise problem has been obviated with an inexpensive and simple RF shield.

Field Stabilization In most MRI systems, the dominant system noise enters through the receiver system. Because PMRI uses an electromagnet readout magnet, the stability of the main magnetic field is equally problematic. Any noise superimposed on the magnetic field behaves identically to phase noise of an oscillator placing a maximum limit on achievable SNR. We have constructed and tested our first stabilization circuitry using a dual feedback topology, to stabilize a Sorenson DCR 300-33T 10 kW power supply. The basic topology

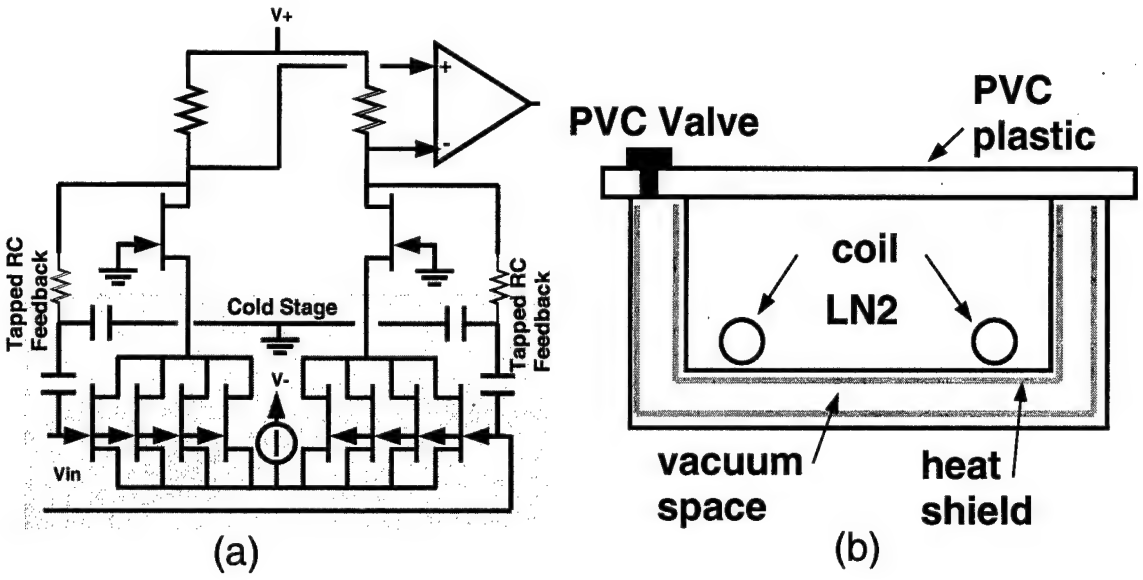

Figure 7: (a)Differential Cascode preamp with cold front end and split RC feedback networks are implemented with U431 JFETs. (b) Dewar redesign to use PVC tube and vacuum for basic liquid nitrogen cooled coil.

and measured regulation are shown in Fig. 6. We achieved up to 70 dB attenuation of error currents. Measured noise spectra of 60Hz harmonics indicated field devations of under 5 ppm - an interference level that is unobservable unless signal SNR exceeds 100. These results were presented at the May 1999 ISMRM in Philadelphia.

Cryo-Preamplifier Our initial proposal called for a combined HTS coil and single ended preamplifier with a novel split capacitor-resistor feedback for low noise damping. For our first designs, we instead selected LN2 copper for flexibility in prototyping, and concentrated on refining our preamplifier architecture for both low noise, and to minimize external electric field interference effects. We have devised a balanced differential input stage that eliminates the need for passive balun between receiver coil and preamp and employs a dual tapped capacitor feedback for the differential pair (Fig. 7 left) . This construction was needed to prevent the existence of unbalanced currents in the signal path from degrading system SNR. The input devices are paralleled JFETs (U431) whose number is chosen to bring the current noise "ceiling" to within the maximum tuned impedance of the receiver coil. These devices form the first part of a differential cascode stage submersed in liquid nitrogen, with the remainder of the cascode connected via micro-coax at room temperature.

Initially, we had considered using a G-10 fiberglass and foam dewar to contain the preamp and coil, but recent developments have indicated that a PVC plastic would be less expensive and superior. Fig. 7, right, shows the design. Concentric PVC tubing forms the dewar, with a vacuum space between, and thin metallized mylar forming a heat radiation shield. The mylar is stripped to prevent eddy current losses but does provide extra electric field shielding. The vacuum levels are not critical with even 1 hour hold time being adequate. This approach is cheaper and less wasteful of the available imaging volume.

7 Key Research Accomplishments

Our key research accomplishments this year were:

1. During the first year of the project, we developed a fast algorithm for homogeneous magnet design using linear programming. The graduate student on the project, Hao Xu, wrote a paper describing the algorithm and that was recently accepted by the IEEE Transactions on Magnetics. A copy of the manuscript is included for your reference.

2. Developed, tested, and refined L1-norm optimization software to design the coil layout for a homogeneous mammography magnet.

3. Using the magnet design software developed above, we were able to discover fundamental scaling limits for both resistive and superconducting magnets. Because our new algorithm is extremely fast (a few seconds per magnet), we were able to design hundreds of magnets spanning all possible magnet lengths and bore sizes. We found that for each bore size, there is an optimal length magnet. A magnet constrained to be shorter than the optimal length requires exponentially more magnet power. And we found there is no advantage for magnets longer than the optimal length. This extremely powerful scaling law was an oral presentation by our graduate student, Hao Xu, at the 1999 ISMRM.

4. Designed and tested two redundant versions of software to model thermal properties of homogeneous magnets, including convective and conductive heat transfer mechanisms.

5. Designed an edge-cooling system for a 12-inch bore homogeneous electromagnet that restricts the temperature variation between coils to less than 10 C. This system has been put into CAD/CAM and will be implemented by Alpha Magnetics within the next month.

6. Developed and redundantly simulated an inexpensive and simple shimming technique using resistors. This is also part of the Alpha Magnetics quote.

7. Installed an 8 by 8 by 10 foot RF magnetic screen room in our lab in the basement of the new Packard Electrical Engineering Building. Fortunately this screen room was loaned to us indefinitely by another group in the school engineering. We measured the RF attenuation of the screen room to better than 65 dB. The screen room would have cost at least $10,000.

8. Last summer and early fall, we constructed and tested a switched resonant power supply using IGBTS. After further testing, we presented a talk last May at the 1999 Meeting of the International Society for Magnetic Resonance in Medicine (ISMRM). This new switching supply allows us to reliably pulse the polarizing field to 0.4 T (100 amperes). And it cost less than $500 in capital expenses. We are now scaling up the switch to handle a 40-cm bore polarizing magnet.

9. We recently completed the engineering specification for a water-cooled, head-sized polarizing magnet. Alpha Magnetics submitted us a bid to build the magnet for just $11,000. We recently accepted their bid and Stanford approved the Purchase Order, with delivery expected by late fall. The new magnet is large enough to image a head. Our current hand-sized polarizing magnet has only a 13-cm bore, so this represents a

significant increase in power, cost and mass, which all scale cubically with bore size. This polarizing magnet will fit outside of the 30-cm free bore readout magnet described above.

10. Greig Scott had designed and constructed an ultra-stable current regulator during Year 1. After a significant debugging and testing effort this year, Greig was able to report his successful work at the 1999 ISMRM. This ultra-precise regulator stabilizes the readout current to better than a few parts per million. And the total hardware costs was less than $500.

11. We finalized specifications for a new equi-radius 3 MHz readout magnet with a 30-cm free bore. The magnet has been ordered from Alpha Magnetics. This magnet has a free bore more than double our hand imaging magnet, and water cooling so that it can operate at 3 times the field strength, or nine times the power. To accommodate these upgrades, we significantly simplified the overall mechanical design by using resistive shims instead of plate-mounted coils. Despite the significant upgrades, Alpha Magnetic's bid ($6,720) is only 40% of the cost of our hand-sized readout magnet ($17,000). Hence, we are extremely encouraged with our progress.

12. The readout magnetic field must be stable to within a few parts-per-million (ppm) during the 100-200 ms readout interval. But the field may be turned off during the 0.8 to 2 second polarizing interval. Currently we use an expensive ($9,000) DC current supply rated for the peak power. Exploiting the low duty cycle of the readout magnet, we can actually supply a 3 MHz center frequency for less than 500 W, which is easily supplied by a standard wall outlet. Two undergraduate research assistants (Alex Tung and Ross Venook) studied a feedback regulator that could cost as little as $1000. We intend to have Alpha Scientific Electronics construct the new switched stable supply.

13. We also had another undergraduate research student (Jack Wang) work with us this summer to port our custom automatic Field Mapping software onto a PC running Linux. Jack wrote some C routines to control a 2-axis motion controller (through an RS-232 interface) and an ESR magnetometer with ppm accuracy (through a GPIB interface). The field plotting functionality was recently successfully tested in the new Packard Electrical Engineering building. Next, we need to machine a pair of mounting plates to precisely guide the ESR probe along the magnet axis. Our goal is to have this completely tested so that we can shim our new 30-cm bore readout magnet when it arrives in 4 weeks.

14. We have modified the linear programming algorithm developed in Year 1 to design transverse and axial Gradient coils. We believe this is the only algorithm that allows for the gradient coil former surface to be completely arbitrary. It is also extremely fast (about 2 minutes computation time), and generates a gradient coil with a minimum complexity. Hao Xu presented this work at the 1999 ISMRM. Following our fundamental work in homogeneous magnet scaling, we hope to find similar scaling rules for gradient coils. This will give us general rules of thumb on constrained length gradients, a very important part of PMRI system design.

15. An undergraduate research assistant, David Pai, spent the summer optimizing construction methods for the gradient coils described above. We found that we can build our

own gradient coils in the lab using copper tape and mylar insulation over a stencil that we laser printed onto a plastic sheet. We then mount the sheet onto an acrylic former, with total expenses less than $100. Out first gradient coil was about half as long as the classic Golay set.

16. We built, debugged and successfully tested a digital interface between the TECMAG console and the polarizing voltage supply. This allows us 5-bit control over the polarizing current directly from the TECMAG pulse sequence editor. Mike Ross, one of our undergraduates has begun a printed circuit board layout of the wire-wrap circuit.

17. We determined that the presence of the polarizing magnet should not effect image quality provided that we design the polarizing coil radius to be about 50% larger than the radius of the receiver coil. We also found that transients induced in the readout magnet by the switching of the polarizing magnet are brief enough that they should cause no image artifacts. These findings are critical to overall system integration.

8 Reportable Outcomes

1. "Homogeneous Magnet Design Using Linear Programming," Hao Xu, Steven Conolly, Greig Scott, Albert Macovski, *accepted by IEEE Transactions on Magnetics*, August 1999.

2. "Minimum Power Homogeneous Magnet Design for Prepolarized MRI," H. Xu, S.M. Conolly, G. Scott and A. Macovski, *Proceedings of the ISMRM*, p. 2006, 1998.

3. "Polyphase Techniques for Low Cost MRI Receivers," G. Scott, S. Conolly and A. Macovski, *Proceedings of the ISMRM*, p. 2020, 1998.

4. "Minimum-Cost Solenoid Design for Prepolarized MRI," S.M. Conolly, G.C. Scott and A. Macovski. *Proceedings of the ISMRM*, p. 255, 1998.

5. "Fundamental Scaling Relations for Homogeneous Magnets," H. Xu, S.M. Conolly, G.C. Scott and A. Macovski. *Proceedings of the ISMRM*, p. 475, 1999.

6. "Gradient Design with Arbitrary Geometrical Constraints by Linear Programming," H. Xu, S.M. Conolly, G.C. Scott and A. Macovski. *Proceedings of the ISMRM*, p. 747, 1999.

7. "Coaxial Stub Matching Strategies for Intravascular Coils," G.C. Scott, P.A. Rivas, and A. Macovski. *Proceedings of the ISMRM*, p. 2070, 1999.

8. "A High-Power Pulsing Circuit for Prepolarized MRI," S.M. Conolly, N.I. Matter, G.C. Scott and A. Macovski. *Proceedings of the ISMRM*, p. 473, 1999.

9. "Electromagnet Current Regulation with Thyristor Supplies," G.C. Scott, H. Xu, S.M. Conolly, A. Macovski. *Proceedings of the ISMRM*, p. 743, 1999.

10. "Design of Dedicated Shim Fields," E. Adalsteinsson, S.M. Conolly, H. Xu, A. Macovski. *Proceedings of the ISMRM*, p. 477, 1999.

11. Patent Application: Hao Xu, Steven Conolly, "Method for Designing Electromagnets having Arbitrary Geometrical Constraints," filing date 5/21/99. Stanford Ref: S99-056. U.S. Application Number 09/316,738. This patent application describes a general algorithm for designing electromagnets with arbitrary former constraints. We have found this to be very useful for low-cost magnet design, but there has been no effort yet to commercialize.

12. Patent Application: Hao Xu, Steven Conolly, Bob Hu "Short Bore-Length Asymmetric Electromagnets for MRI," field 5/21/99. U.S. Application number 09/316,530. Stanford Ref: S99-057. This is a patent for a particular magnet with better patient and physician access. No effort yet to commercialize.

13. This exciting biomedical engineering project has provided undergraduate research opportunities for seven undergraduate students at Stanford this year including Ross Venook, Dave Pai, Alex Tung, Jack Wang, Karen Tisdale, Jaime Wong, Mike Ross and Lexyne McNealy. Lexyne is a visting student from Spelman College. The first four students were studying under a Stanford research award called the REU program.

9 Conclusions

The bid from Alpha Magnetics is quite encouraging since it proves that the two principal magnets for a *patient-sized* PMRI system can indeed be constructed for just $20,000. The remaining costs include: the gradient coil amplifiers (about $3,000), the readout pulsed power supply (about $1,000), and the polarizing switcher (about $4,000). The Tecmag system console cost $48,000, but we believe this PC-based controller could be produced wholesale for less than $5,000 in hardware. Indeed, Greig Scott from our group gave a talk at the 1999 ISMRM on inexpensive digital MRI receivers. Hence, we have verified that the capital costs are less than $40,000, significantly less than the $400,000 capital cost of a conventional high-field MRI scanner.

What remains is system integration and testing to ensure that the image quality is as good as conventional scanners. That is our goal for the coming year. We were very fortunate to be able to recruit Blaine Chronik, who recently was awarded a prestigious Canadian NSERC postdoc fellowship, to help us with system integration. Blaine is currently one of the top graduate students developing MRI hardware in the world. He will be of enormous help in the coming year.

References

[1] M. J. E. Golay, Field homogenizing coils for nuclear spin resonance instrumentation, *Rev. Sci. Instrum.*, **29**, 313, (1958).

[2] J. R. Baker, An improved three-coil system for producing a uniform magnetic field, *J. Sci. Instrum.*, **27**, 197, (1950).

[3] M. W. Garrett, Calculation of fields, forces and mutual inductances of current system by elliptic integrals, *J. Appl. Phys.*, **34**, 2567, (1963).

[4] M. Garrett, Thick cylindrical coil systems with field or gradient homogeneities of the 6th to 20th order, *J. Appl. Phys.*, **38**(6), 2563–2586, (1967).

[5] G. Grossl, F. Winter, and R. Kimmich, Optimisation of magnet coils for NMR field-cycling experiments, *Journal of Physics E*, **18**, 358, (1985).

[6] H. Saint-Jalmes and J. Taquin, Optimization of homogeneous electromagnetic coil systems: Application to whole-body NMR imaging magnets, *Rev. Sci. Instrum.*, **52**, 1501, (1981).

[7] K. Kaminishi and S. Nawata, Practical method of improving the uniformity of magnetic fields generated by single and double Helmholtz coils, *Rev. Sci. Instrum.*, **52**, 447, (1981).

[8] R. Merritt, C. Purcell, and G. Stroink, Uniform magnetic field produced by three, four, and five squared coils, *Rev. Sci. Instrum.*, **54**, 879, (1983).

[9] J. V. Bladel, "Electromagnetic Fields". Hemisphere, New York, 1985.

[10] R. Turner, A target field approach to optimal coil design, *J. Phys. E: Scientific Instruments*, **19**, 147–151, (1986).

[11] M. Engelsberg, R. E. de Souza, and C. M. D. Pazos, The limitations of a target field approach to coil design, *Journal Physics D-Applied Physics*, **21**(7), 1062–1066, (1988).

[12] D. I. Hoult and R. Deslauriers, Accurate shim-coil design and magnetic field profiling by a power-minimization-matrix method, *J. Magn. Reson.*, **108**, 9, (1994).

[13] S. Pissanetzky, Structured coils for NMR applications, *IEEE Trans. Mag.*, **28**, 1961, (1992).

[14] M. D. Ogle and J. D'Angelo, Design optimization method for a ferromagnetically self-shield MR magnet, *IEEE Trans. Mag.*, **27**, 1689, (1991).

[15] H. Siebold, H. Huebner, L. Soelsner, and T. Reichert, Performance and results of a computer program for optimizing magnets with iron, *IEEE Trans. Mag.*, **24**, 419, (1988).

[16] G. Drago, A. Manella, M. Nervi, M. Repetto, and G. Secondo, A combined strategy for optimization in non-linear magnetic problems using simulated annealing and search techniques, *IEEE Trans. Mag.*, **28**, 1541, (1992).

[17] S. Noguchi and A. Ishiyama, Optimal design method for MRI superconducting magnets with ferromagnetic shield, *IEEE Trans. Mag.*, **33**, 1904, (1997).

[18] A. Ishiyama, K. Shimizu, and A. Sakahara, An optimal design method for multi-section superconducting magnets using modified simulated annealing, *IEEE Trans. Mag.*, **30**, 3435, (1994).

[19] M. Kitamura, S. Kakukawa, K. Mori, and T. Tominaka, An optimal design technique for coil configuraions in iron-shielding MRI magnets, *IEEE Trans. Mag.*, **30**, 2352, (1994).

[20] A. K. Kalafala, A design approach for actively shielded MRI magnets, *IEEE Trans. Mag.*, **26**, 181, (1990).

[21] A. K. Kalafala, Optimized configuration for actively shielded MRI magnets, *IEEE Trans. Mag.*, **27**, 1696, (1990).

[22] F. J. Davies, R. T. Elliott, and D. G. Hawksworth, A 2-Tesla active shield magnet for whole body imaging and spectroscopy, *IEEE Trans. Mag.*, **27**, 1677, (1991).

[23] D. G. Hawksworth, I. L. McDougall, and J. M. Bird, Considerations in the design of MRI magnets with reduced stray field, *IEEE Trans. Mag.*, **23**, 1309–1314, (1987).

[24] H. Xu, S. Conolly, G. Scott, and A. Macovski, Minimum power homogeneous magnet design for prepolarized MRI, *in* "Proceedings of the ISMRM", p. 2006, March 1998.

[25] H. Xu, S. Conolly, G. Scott, and A. Macovski, Minimum power homogeneous magnet design for prepolarized MRI, *in* "Experimental NMR Conference", p. 33, April 1998.

[26] H. Xu, S. Conolly, G. Scott, and A. Macovski, Minimum power homogeneous magnet design for prepolarized MRI, *in* "ISMRM Workshop on Electromagnetics in MRI", May 1998.

[27] P. E. Gill, W. Murray, and M. H. Wright, "Practical Optimization". Academic Press, London, 1981.

[28] L. B. Lugansky, Optimal coils for producing uniform magnetic fields, *Rev. Sci. Instrum.*, **39**, 1372, (1986).

[29] L. B. Lugansky, On optimal synthesis of magnetic field, *Rev. Sci. Technol.*, **1**, 53, (1990).

[30] D. B. Montgomery, "Solenoid Magnet Design". Krieger, Malbar, Florida, 1969.

[31] P. Morgan, S. Conolly, G. Scott, and A. Macovski, A readout magnet for prepolarized MRI, *Magnetic Resonance in Medicine*, **36**(4), 527–36, (1996).

[32] D. Korbee et al., Magnet system for very low field imaging, *in* "Proceedings of the Society of Magnetic Resonance", p. 933, August 1995.

10 Appendices

The next two pages show copies of the blueprints for the resistive 12-inch bore electromagnet being constructed by Alpha Magnetics.

The first shows a two-vent cooling design for our latest 12-inch bore readout magnet. Each cooling unit has one or two turns of refrigerator tubing, a 5 mil copper thermal diffuser and an electrical insulator (not visible). The cooling unit is epoxied to the coil surface. Note that care has been taken to avoid eddy current paths in the copper cooling elements.

The second blueprint shows our latest 12 inch bore readout magnet to test the resistive shimming idea. Note that each of the six coils is broken in two to allow for separate shimming of radial variations. In our first magnet, we found that the outer radius of the magnet varied by up to 50 mils due to accumulations in winding errors. We have determined that this method will allow us to shim out variations of even 100 mils using very inexpensive resistors.

We also include a preprint of of Hao Xu's accepted paper on magnet design.

FIGURE 1

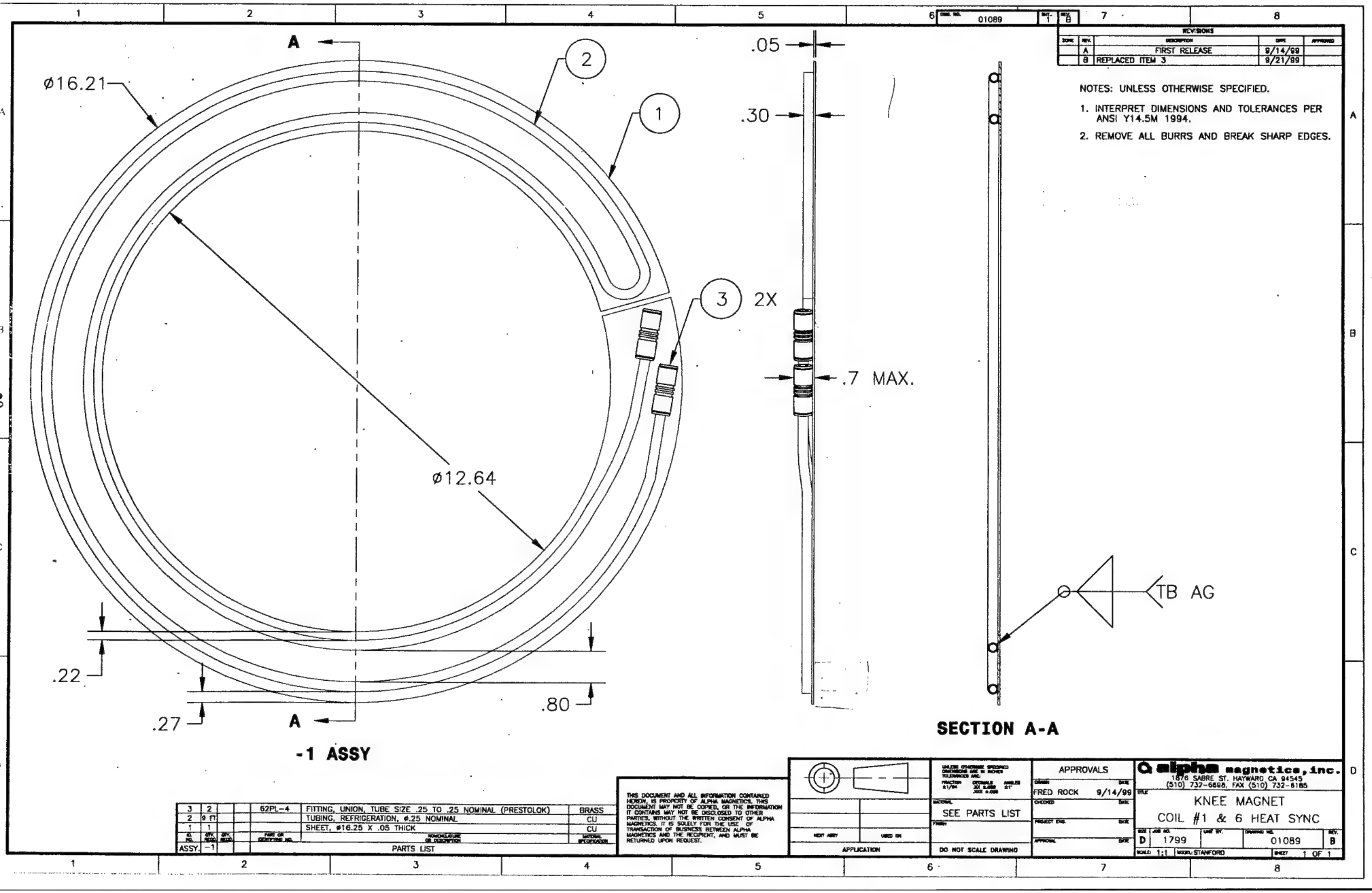
A
ø16.21
2
1
3 2X
ø12.64
.22
.27
.80
A
-1 ASSY
.05
.30
.7 MAX.
TB AG
SECTION A-A
NOTES: UNLESS OTHERWISE SPECIFIED.
1. INTERPRET DIMENSIONS AND TOLERANCES PER ANSI Y14.5M 1994.
2. REMOVE ALL BURRS AND BREAK SHARP EDGES.
REVISIONS
A FIRST RELEASE 9/14/99
B REPLACED ITEM 3 9/21/99
3 2 62PL-4 FITTING, UNION, TUBE SIZE .25 TO .25 NOMINAL (PRESTOLOK) BRASS
2 9 ft TUBING, REFRIGERATION, ø.25 NOMINAL CU
1 1 SHEET, ø16.25 X .05 THICK CU
ASSY. -1
PARTS LIST
THIS DOCUMENT AND ALL INFORMATION CONTAINED HEREIN, IS PROPERTY OF ALPHA MAGNETICS. THIS DOCUMENT MAY NOT BE COPIED, OR THE INFORMATION IT CONTAINS MAY NOT BE DISCLOSED TO OTHER PARTIES, WITHOUT THE WRITTEN CONSENT OF ALPHA MAGNETICS. IT IS SOLELY FOR THE USE OF TRANSACTION OF BUSINESS BETWEEN ALPHA MAGNETICS AND THE RECIPIENT, AND MUST BE RETURNED UPON REQUEST.
APPROVALS
FRED ROCK 9/14/99
SEE PARTS LIST
DO NOT SCALE DRAWING
alpha magnetics, inc.
1676 SABRE ST. HAYWARD CA 94545
(510) 732-6898, FAX (510) 732-6185
KNEE MAGNET
COIL #1 & 6 HEAT SYNC
D 1799 01089 B
SCALE: 1:1 WEIGHT: STANFORD SHEET 1 OF 1

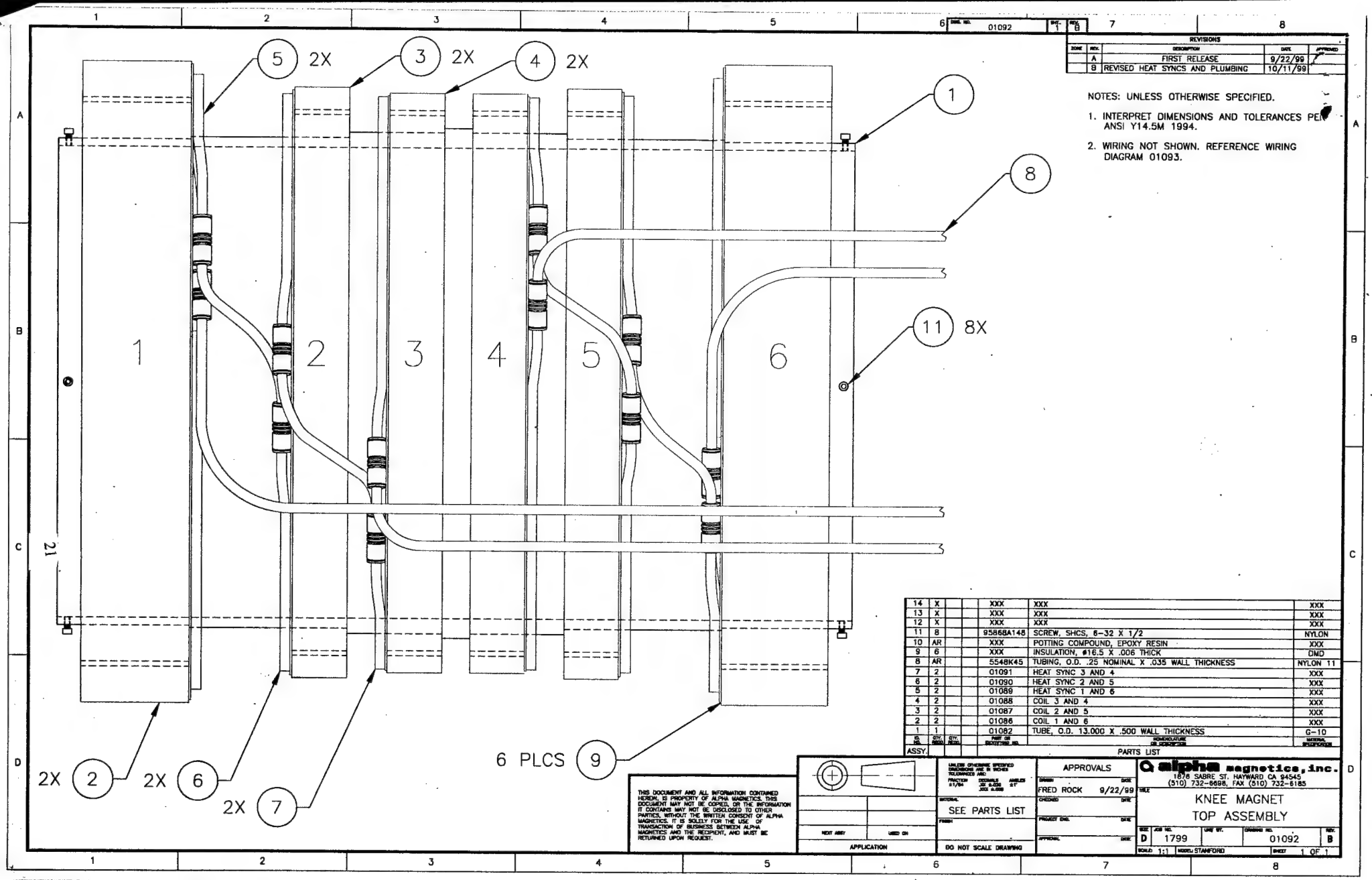

REVISIONS				
ZONE	REV.	DESCRIPTION	DATE	APPROVED
	A	FIRST RELEASE	9/22/99	
	B	REVISED HEAT SYNCS AND PLUMBING	10/11/99	

NOTES: UNLESS OTHERWISE SPECIFIED.

1. INTERPRET DIMENSIONS AND TOLERANCES PER ANSI Y14.5M 1994.
2. WIRING NOT SHOWN. REFERENCE WIRING DIAGRAM 01093.

ITEM NO.	QTY. REQD.	QTY. REVD.	PART OR IDENTIFYING NO.	NOMENCLATURE OR DESCRIPTION	MATERIAL SPECIFICATION
14	X		XXX	XXX	XXX
13	X		XXX	XXX	XXX
12	X		XXX	XXX	XXX
11	8		95868A148	SCREW, SHCS, 6-32 X 1/2	NYLON
10	AR		XXX	POTTING COMPOUND, EPOXY RESIN	XXX
9	6		XXX	INSULATION, ø16.5 X .006 THICK	DMD
8	AR		5548K45	TUBING, O.D. .25 NOMINAL X .035 WALL THICKNESS	NYLON 11
7	2		01091	HEAT SYNC 3 AND 4	XXX
6	2		01090	HEAT SYNC 2 AND 5	XXX
5	2		01089	HEAT SYNC 1 AND 6	XXX
4	2		01088	COIL 3 AND 4	XXX
3	2		01087	COIL 2 AND 5	XXX
2	2		01086	COIL 1 AND 6	XXX
1	1		01082	TUBE, O.D. 13.000 X .500 WALL THICKNESS	G-10

ASSY. PARTS LIST

THIS DOCUMENT AND ALL INFORMATION CONTAINED HEREIN, IS PROPERTY OF ALPHA MAGNETICS. THIS DOCUMENT MAY NOT BE COPIED, OR THE INFORMATION IT CONTAINS MAY NOT BE DISCLOSED TO OTHER PARTIES, WITHOUT THE WRITTEN CONSENT OF ALPHA MAGNETICS. IT IS SOLELY FOR THE USE OF TRANSACTION OF BUSINESS BETWEEN ALPHA MAGNETICS AND THE RECIPIENT, AND MUST BE RETURNED UPON REQUEST.

NEXT ASSY | USED ON | APPLICATION

UNLESS OTHERWISE SPECIFIED DIMENSIONS ARE IN INCHES. TOLERANCES ARE: FRACTION ±1/64 | DECIMALS .XX ±.030 .XXX ±.005 | ANGLES ±1°

MATERIAL: SEE PARTS LIST

FINISH:

DO NOT SCALE DRAWING

APPROVALS		
DRAWN	FRED ROCK	9/22/99
CHECKED		
PROJECT ENG.		
APPROVAL		

alpha magnetics, inc.
1878 SABRE ST. HAYWARD CA 94545
(510) 732-8898, FAX (510) 732-8185

TITLE: KNEE MAGNET TOP ASSEMBLY

SIZE	JOB NO.	WT.	DRAWING NO.	REV.
D	1799		01092	B

SCALE: 1:1 | MODEL: STAMFORD | SHEET 1 OF 1

FIGURE 2

Homogeneous Magnet Design Using Linear Programming

Hao Xu, Steve Conolly, Greig Scott, Albert Macovski

Abstract— **In this paper, we introduce a technique for designing homogeneous magnets using linear programming. We first show that minimum-power homogeneous magnet design can be cast as a linear programming problem. We also show that the method is applicable to minimum conductor mass superconducting magnet design. The method has several advantages over existing techniques including: it allows complete flexibility in arbitrary geometric constraints on both the coil locations and the shape of the homogeneous volume; it guarantees a globally optimal solution; rapid computation speed (≈ 30 s). Three resistive magnet design examples and one shielded superconducting magnet design are presented to illustrate the flexibility of the method.**

Keywords— **Magnet design, Linear Programming, MRI, Prepolarized MRI.**

I. Introduction

HOMOGENEOUS magnet design techniques using discrete current loops date back to the classic papers of McKeehan, Garrett and others [1], [2], [3], [4], [5], [6], [7], [8]. These papers described precise coil arrangements designed to cancel as many lower-order spherical harmonics of the B field as possible. These classic analytic techniques were used to design solenoidal magnets with spherically shaped homogeneous volumes for applications such as bubble chamber magnets for particle detection, or magnets for chemical analysis by NMR [4], [9]. These methods rely on analytic expressions for the field from each coil, so they are limited to coils assembled on the surface of a cylinder or a sphere.

Due to the high field strength and large homogeneous volume required, magnet design techniques tailored to MRI have focused on superconducting magnets with iron shielding [9], [10], [11], [12], [13], [14] or actively shielded magnets [15], [16], [17], [18], [19], [20]. Most early magnet designs were four or six-coil equi-radius whole body magnets. Recently there has been a surge of interest in dedicated MRI scanners for applications such as head imaging and musculoskeletal imaging. These applications demand more open magnet designs tailored to the body part.

Our group has also been developing a new concept in low-cost MRI called Prepolarized MRI (PMRI). Prepolarized MRI requires two resistive magnets. First, a strong (0.5 – 1 T) but non-uniform "polarizing" magnet magnetizes the volume. The polarizing magnet is switched off quickly, and a second homogeneous but weaker (50 – 100 mT) "readout" magnet remains on during the excitation and imaging phase. Hence it governs a much lower center frequency (about 2 to 6 MHz) for signal readout. Provided tissue noise dominates coil noise for the low frequency readout, the SNR and contrast should be identical to a conventional MRI scanner with field equal to the polarizing field. However, the cost is greatly reduced with a PMRI approach since both magnets can be resistive. PMRI systems require integration of two magnets into a single, low-cost system, while maximizing patient access and comfort. Hence, readout magnet design for PMRI must maximize flexibility of the coil layout while minimizing power consumption.

This work is supported by research grants from the Whitaker Foundation (176W156), the California Tobacco-Related Disease Research Program (6RT-0384), the ARMY BCRP program (DAMD17-98-1-8157), and the NIH R21 program(R21 HL60328-01).

The authors are with the Dept. of Electrical Engineering, Stanford University, Stanford, CA

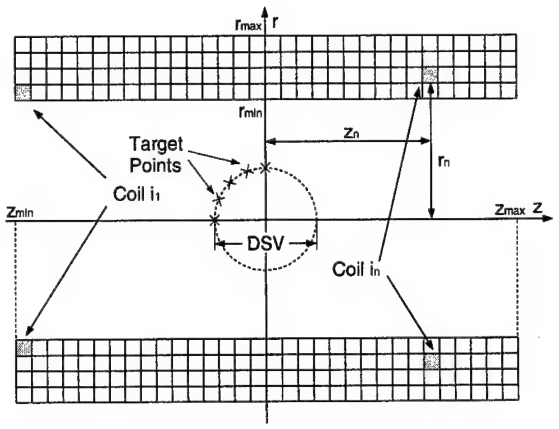

Fig. 1. The magnet design problem. The feasible coil space is densely sampled by an array of candidate coils. The coils are assumed to be ideal current loops located at the center of the squares. The goal is to pick the right coils and currents to create a homogeneous field at the target points while minimizing the magnet power. The shape of homogeneous volume and the feasible set of coils are entirely arbitrary.

To address the need for magnet design with arbitrary coil positions and arbitrarily shaped homogeneous volumes, many new magnet design approaches have been proposed. Unlike classic techniques, more recent techniques have relied on numerical optimization to generate magnets with far greater geometrical flexibility [21]. These techniques enumerate all feasible coil location and radii to search for the optimal coil and current combination.

Fig. 1 illustrates the homogeneous magnet design problem. We must find a small number of coils that can generate a magnetic field with specified homogeneity over the imaging region. Each coil is defined by its current, i_n, its radii, a_n, and its z location, z_n. Note the coil z location and radii are nonlinearly related to the B field while the coil currents are linearly related to B. We insist on a practical magnet design that uses fewer than, say, a dozen of

the feasible coils.

Many approaches treat this as a general nonlinear optimization problem, especially when magnetic materials are present. Powerful but relatively slow numerical methods such as simulated annealing are applied to iteratively optimize the magnet design and these algorithms typically minimize the field error and/or conductor cost [22], [23], [24], [25]. In 1986, Lugansky used nonlinear optimization to find a set of N coils that minimized the mean-squared field error [26], [27].

In 1992, Pissanetzky introduced a method that minimized the mean-squared field error subject to hard constraints on the magnitude of the currents [28]. His optimal currents gravitated towards the peak magnitude. He called the magnets "structured," since clusters of adjacent currents all have the same current direction. He believes structured magnets could be built with a modified series winding by simply changing the winding direction for each new current direction. This method is powerful and flexible, but reduces the magnet length by increasing magnet power or cost. Hence, we were motivated to find a method that directly minimizes cost or power rather than field error.

There are also several methods using linear matrix approaches to solve the magnet design problem. These algorithms can be very efficient, and in theory should always reach a globally optimal solution. However, it has been quite difficult for researchers to find practical "buildable" magnets. Linear methods attempt to invert the matrix relationship relating the field $\mathbf{b}$ at the M target points to the currents $\mathbf{i}$ in the N feasible coils.

$$\mathbf{b} = A\,\mathbf{i} \tag{1}$$

where A_{mn} is the field at the m^{th} target point due to a unit current in the n^{th} feasible coil. Direct matrix inversion is difficult since the matrix $\mathbf{A}$ is very poorly conditioned. Turner in 1986 and Thompson in 1994 performed an analogous inversion using Fourier domain approaches [29], [30]. Engelsberg pointed out that these methods can sometimes yield "very complex and strongly peaked current distributions" [31]. Hoult and Deslauriers used a pseudo-inverse to solve this problem [32]. Schweikert et al., inverted the matrix analytically [33]. But the magnets generated by these method typically require non-zero currents in nearly all of the feasible coils, which makes magnet construction difficult.

In 1996, Morgan et al., described a magnet design algorithm called "subset selection." Here, a small, predetermined number (N_{ss}) of coils were preselected by picking the N_{ss} most linearly independent columns of the $\mathbf{A}$ matrix [34], [35]. He collected the N_{ss} columns into a reduced dimension matrix, which is much better conditioned, so that the pseudo-inversion technique can then be used to find minimum-power currents. This technique is relatively fast and completely flexible for the coil layout and homogeneous volume geometry, but the level of inhomogeneity cannot be effectively controlled and the number of coils is not automatically chosen. Furthermore, because of the two-step optimization, very little can be said about the global optimality of this algorithm.

Ideally, we would like a fast algorithm for designing homogeneous magnets that allows for arbitrary constraints on both coil placement and on the shape of the homogeneous volume. The algorithm should also automatically choose the minimum number of coils necessary for the constraints.

Below we introduce a method that minimizes magnet power subject to maximum field error constraints [36], [37]. We believe the new approach offers significant advantages over existing magnet design algorithms for designing resistive and superconducting homogeneous magnets. We first show that the magnet design problem can be solved very efficiently using Linear Programming. Then we illustrate the flexibility of the method with three resistive magnet design examples and one minimum-cost shielded superconducting magnet example.

II. Problem Formulation and Implementation

We begin with the magnet design problem illustrated in Fig. 1. A dense array of *candidate* coils are shown covering the feasible coil space. We typically use 50 to 100 coils to ensure adequate spatial resolution. For initial calculations, the field generated by each coil is approximated by the field from an ideal current loop (with zero cross sectional area) located at the center of the of the grid cell. It is important to note that the grid size shown in the figure only defines the separation between neighboring candidate coils; it does not define the coils' cross section, which could actually be larger than the grid cell size. An arbitrarily shaped homogeneous volume is specified by a set of target points on the surface of the volume. We constrain the magnetic field to be uniform at these target points. The most common shape is spherical (as shown in the figure), which is typically defined by its diameter, DSV, meaning "Diameter Spherical Volume."

In MRI, the field *magnitude* governs both magnetization intensity and reception frequency. Fortunately, we need to constrain only the homogeneity of the B_z component to ensure homogeneity of the field magnitude within a homogeneous volume. For a system of coaxial circular coils, only the B_z and B_r fields need to be considered. Here we show that to force the field magnitude to be homogeneous, one only needs to constrain B_z.

Let us break the two field components into their desired field plus residual terms with relative errors ϵ_r and ϵ_z,

$$\begin{aligned} B_z &= B_0 + \epsilon_z B_0 \\ B_r &= \epsilon_r B_0 \end{aligned} \tag{2}$$

Then the magnitude of the field is

$$|B| = \sqrt{B_z^2 + B_r^2} \;= B_0\sqrt{(1+\epsilon_z)^2 + \epsilon_r^2} \tag{3}$$

Because ϵ_r is much smaller than 1, it will have negligible contribution to the $|B|$. This effect is often called quadrature suppression. Garrett showed that ϵ_z and ϵ_r are within an order of magnitude in a homogeneous magnet [4]. Hence

we can always neglect the radial component of the field when the B_z field is homogeneous.

Each coil generates a magnetic field contribution at each target point. If the n^{th} coil has radii r_n, and z location z_n, and current i_n, then the B_z field per unit current generated at the m^{th} target point (ρ_m, ζ_m) is [38]

$$A_{mn} = \frac{\mu}{2\pi[(r_n+\rho_m)^2+(\zeta_m-z_n)^2]^{1/2}} \left[K(\kappa_{mn}) + \frac{r_n^2-\rho_m^2-(\zeta_m-z_n)^2}{(r_n-\rho_m)^2+(\zeta_m-z_n)^2}E(\kappa_{mn})\right], \quad (4)$$

where the functions $E()$ and $K()$ are complete elliptic integrals of the first and second kind, and the κ_{mn} is defined as

$$\kappa_{mn} = \left(\frac{4r_n\rho_m}{(r_n+\rho_m)^2+(\zeta_m-z_n)^2}\right)^{1/2} \quad (5)$$

The field B_z at the m^{th} target point is simply the sum of the magnetic field generated by all the coils. In matrix form, the field at the target points is

$$\mathbf{b} = A\,\mathbf{i} \quad (6)$$

The homogeneity constraints are:

$$|b_m - B_0| \le \epsilon\, B_0, \;\; m = 1\cdots M\,, \quad (7)$$

where ϵ is typically between 1 and 10 ppm. We feel that this constraint is the most prudent for MRI since it does not overspecify the magnet design. Other methods typically enforce homogeneity *equality* constraints at the target points. We believe these other methods overconstrain the design since they implicitly specify the exact locations of the zeros of the inhomogeneity profile. In our experience, this method makes the magnet design independent of the precise target point locations on the target surface.

The M × N matrix A is in general very poorly conditioned since the field contribution due to adjacent coils are quite similar. The vector $\mathbf{i}$ defines the current in each coil. Our goal is to find a (sparse) current vector that generates the desired field with minimum power.

The power dissipated by the magnet is simply the sum of power in each of the coils:

$$P = \sum_{n=1}^{N} |i_n|^2 \left(\frac{2\pi r_n}{\sigma_c S_n}\right), \quad (8)$$

where S_n and r_n are the cross sectional area and radii of the n^{th} coil, respectively. Note that the ratio $|i_n|/S_n$ is simply the current density j_n of the n^{th} coil. We can rewrite the power equation as

$$P = \frac{2\pi}{\sigma_c}\sum_{n=1}^{N} j_n |i_n| r_n\,, \quad (9)$$

We now make an important assumption that the magnet will be implemented with uniform current density. This is always true for series connected magnets with uniform wire size, where the number of turns is proportional to the total current in each coil. With $j_n = J$ the power is

$$P = \frac{2\pi J}{\sigma_c}\sum_{n=1}^{N} |i_n| r_n \quad (10)$$

We conclude that magnet power is the radii-weighted ℓ_1-norm of current vector $\mathbf{i}$. The ℓ_1-norm of a vector is defined as the sum of the absolute value of its components. The ℓ_2-norm is the familiar square root of the sum of squares.

Hence, minimum-power magnet design with field homogeneity inequality constraints is the following optimization problem:

$$\begin{aligned} &\text{Minimize : } \mathbf{r}^{\mathbf{T}}|\mathbf{i}| \\ &\text{Subject to : } B_0\,(1-\epsilon) \le A\,\mathbf{i} \le B_0(1+\epsilon) \end{aligned} \quad (11)$$

This belongs in the general category of *convex* optimization problems, for which extremely efficient programming methods have been developed. In particular, there is a well-known trick for recasting ℓ_1-norm minimization problems into canonical linear programming form. To do this, we introduce the auxiliary variables t_1 through t_N [39].

$$\begin{aligned} \text{Minimize :} \quad & \mathbf{r}^T\mathbf{t} \\ \text{Subject to :} \quad & A\,\mathbf{i} \le B_0(1+\epsilon), \\ & -A\,\mathbf{i} \le -B_0(1-\epsilon), \\ & |i_n| \le t_n, \;\; n = 1\cdots N. \end{aligned} \quad (12)$$

The two optimization problems are equivalent since the t_n are constrained to be no smaller than $|i_n|$. This is the only constraint on the t_n, so when minimizing the sum of t_n it is guaranteed that the t_n will be identical to $|i_n|$.

Note that the new formulation is a canonical Linear Programming problem, which is considerably easier to solve than nonlinear programming problems. Current constraints can also be easily incorporated into this formulation. The LP problem can be solved very efficiently with standard software packages. For example, MATLAB has an `lp()` function that we found can handle 50 candidate coils with over 100 target points and compute the minimum power magnet in less than 12 seconds on a SUN Ultra 2. The time increases to 85 seconds for 100 candidate coils. For larger arrays of feasible coils, more sophisticated LP algorithms offer greater speed. We have successfully optimized magnets from 1000 candidate coils using an interior-point predictor-corrector linear programming software package called PCx [40]. We typically use MATLAB's `lp()` for convenience and numerical issues. Below we discuss how 50 to 100 candidate coils gives adequate resolution if iteration is employed judiciously.

As shown in Fig. 1, the candidate coils' radii are constrained between the bounds $r_{\min}$, $r_{\max}$ (which can vary

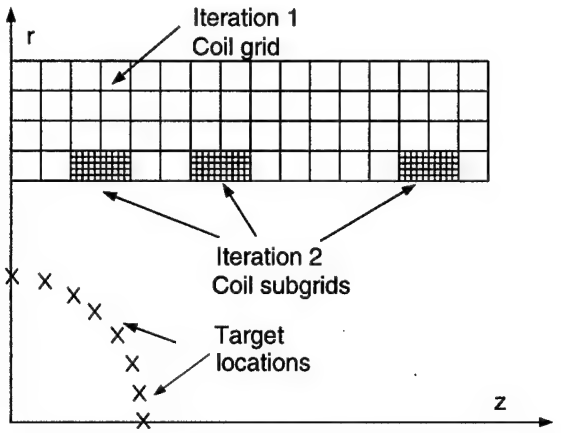

Fig. 2. Iterative magnet design using LP. For this symmetric design, we show only the right half of the magnet. The sparseness of ℓ_1-norm minimization solution allows one to search on successively finer grids for the precise location of coils. Each iteration sets most candidate coils to have zero current. This allows one to specify a finer grid to cover the few non-zero current coils. This process is typically repeated three to four times.

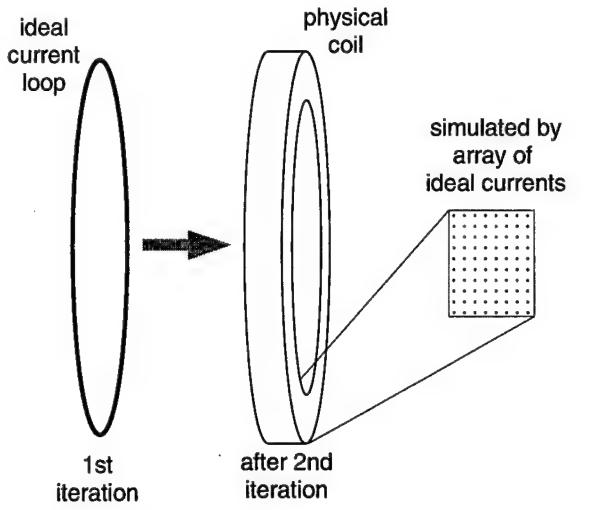

Fig. 3. Iterative improvement of thick coil field modeling. For the first iteration, the coils are assumed to be ideal current loops. For later iterations, the full cross-section of the coils is used to calculate the B field.

with z), and their length is constrained by $z_{\min}$ and $z_{\max}$. All of these constraints are preset by the user. Indeed, iterative adjustment of these constraints quickly becomes a habit. The inner radial bound is typically defined by patient access. The outer radial bounds depend on the application: unshielded magnets typically only use coils at $r_{\min}$ unless the length is severely constrained. Shielded magnets require larger radius feasible coils to generate shielding currents. We typically pick $z_{\max}$ just large enough so that no coils are selected at the bound.

A critical advantage of ℓ_1-norm problems is the *sparseness* of the solution. The solution tends to have the minimum number of non-zero currents required to satisfy the constraints, as shown in Fig. 2. So unlike the matrix inversion methods, this algorithm automatically generates the minimum number of coils necessary to meet the desired homogeneity requirement. This key characteristic makes this method practical.

Of course, with greater coil density one can be more confident that the solution is truly optimal. However, in practice it is best to iterate a few times with a focused array of smaller matrices. On each iteration only 50 to 100 candidate coils are used. Typically, if 6 coils are ultimately required for the magnet design, only 12 candidate coils will have non-zero currents on the first iteration and they come in adjacent pairs, as shown in Fig. 2. We then iteratively focus a finer-resolution grid of coil locations over the previous selected coils. This iteration obtains the precise location of the coils to satisfy the homogeneity requirement. This process is also illustrated in Fig. 2. For a DSV of 20–50 cm, we start with a grid resolution of about 2 cm (about 100 coils). Three to four iterations obtains 0.1 mm precision, which is adequate for most MRI homogeneity requirements.

For the first iteration, we assume the field is the same as that from an ideal current filament located at the center of the coil. The first iteration isolates nonzero coils at a minimum number of locations. Starting with the second iteration, we use the previous iteration's current value to calculate the cross sectional area of each coil. Here, we must assume a current density and a length-to-width ratio for the coils. For the next iteration, we recalculate a more accurate field matrix A incorporating the actual cross section of the coil. To do this we calculate the field from each thick coil by summing the field from a two dimensional sampling array of ideal current loops. This process is illustrated in Fig. 3. The number of elements of the array determines the precision of the calculation. We typically use between 100 and 400 filamentary loops to model a thick coil. If necessary, one can even use the exact wire gauge and number of turns. The accuracy of this procedure was verified along the z-axis using an analytic thick-coil axial field formula [26], [27].

In summary, we have found that minimum-power magnet design can be formulated as a Linear Programming problem. The new magnet design approach offers complete flexibility for handling arbitrary geometric constraints. The algorithm is guaranteed to find the global optimal solution, and it automatically selects the minimum number of coils necessary to satisfy the given constraints. The unprecedented speed of the LP algorithm makes real-time interactive constrained magnet design a reality. In the next section, we illustrate the flexibility of the method with four magnet design examples.

III. Results and Examples

Our new magnet design algorithm is very flexible for handling various arbitrarily shaped homogeneous volumes and coil locations. Here we present several designs that demonstrate its power and flexibility.

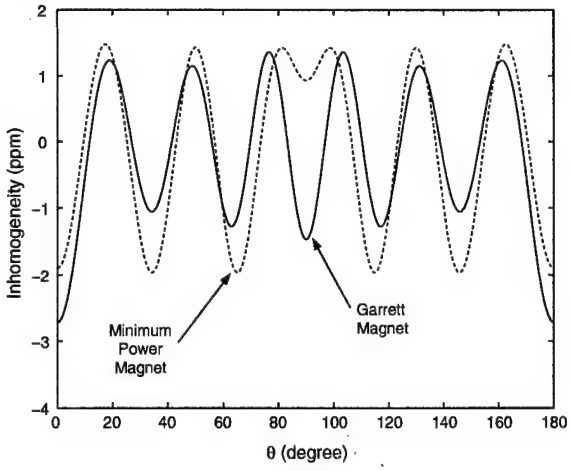

Fig. 4. A comparison of the field inhomogeneity plotted at 6 cm radius for two 30 cm bore magnets: a 6-coil equi-radius Garrett magnet and a minimum-power magnet using identical constraints on length, homogeneity and DSV. The minimum-power designs typically show an equiripple inhomogeneity variation.

A. Garrett Solenoid

As a validity check of our algorithm, we first constructed a magnet using a feasible coil array with radius, homogeneity and DSV designed to match a 6-coil equi-radius magnet with "near maximal power efficiency" from Garrett's classic paper [4]. Our minimum-power algorithm calculated the z_n and i_n. Table I compares the specifications of the minimum-power magnet and the Garrett magnet for B_0 = 23 mT and coil radii, a = 15 cm. The homogeneity profiles for both magnets are plotted in Fig. 4 over a 12-cm DSV. The inhomogeneity is smaller at $\theta = 90$ for the Garrett magnet but grows worse at $\theta = 0$ and $\theta = 180$. Note that the minimum-power magnet has an equiripple inhomogeneity variation. This has always been a characteristic of our technique. We were reassured to find that the Garrett magnet is comparable to our minimum-power magnet in length and power.

TABLE I
SPECIFICATIONS FOR A 6-COIL GARRETT MAGNET AND A COMPARABLE MINIMUM-POWER DESIGN.

	Min. Power	Garrett
power	761.8 W	763.8 W
mass	23.75 kg	23.80 kg
z_1/a	0.159866	0.162553
z_2/a	0.531467	0.537007
z_3/a	1.188600	1.193934
i_1	1.0	1.0
i_2	1.36469	1.34774
i_3	3.50733	3.45517

B. Biplanar Magnet for Mammography

Breast imaging is a possible future application of Prepolarized MRI. A biplanar magnet offers excellent lateral access and could dissipate less power than a solenoid magnet with "equivalent" access, especially given that in a biplanar geometry, one can take advantage of the asymmetry of the imaging anatomy. We set B_0 = 40 mT and ϵ = 10 ppm over a 20 cm DSV. We placed the candidate coils in the regions shown in Fig. 5. The coils were located at z = 15 cm and z = -30 cm with varying radius. We placed the two planes asymmetrically to reduce power dissipation, since the minimum gap between planes would need to be larger for a symmetric design. Here, we cut almost 15 cm in the gap. This illustrates the flexibility of our algorithm for asymmetric magnet design.

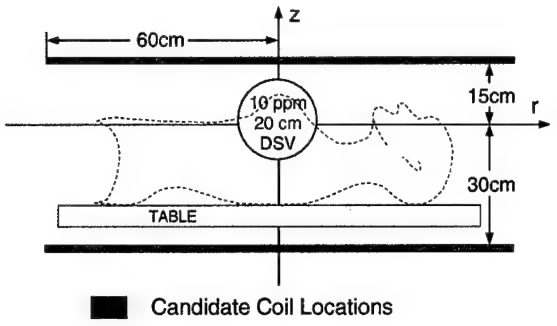

Fig. 5. Candidate coils for biplanar mammography magnet. The candidate coils are allowed 30 cm space below the DSV and just 15 cm above the DSV to conserve power. The coil radii are allowed to vary from 0 to 60 cm.

The minimum-power biplanar design is shown in Fig. 6, and the coil coordinates are presented in Table II. The simulated 10 ppm homogeneous region is calculated from the field magnitude. The coil size is calculated with a 408 A/cm^2 current density. The magnet consists of 6 coils, with two below and four above. It weighs 306 kg and it consumes a power of 9.8 kW at 40 mT. One alternative to this design is a symmetric biplanar magnet with a gap of 60 cm. We designed such a magnet with the LP algorithm and found the power consumption increased 50% to 15 kW. Hence we see the advantage of allowing for completely flexibile coil placement.

TABLE II
SPECIFICATIONS FOR THE MINIMUM-POWER BIPLANAR MAMMOGRAPHY MAGNET SHOWN ABOVE.

	r (cm)	z (cm)	I (A)
Coil 1	51.70	-30.00	20788.4
Coil 2	11.68	-30.00	504.6
Coil 3	4.33	15.00	44.1
Coil 4	9.12	15.00	132.2
Coil 5	17.17	15.00	496.3
Coil 6	52.56	15.00	20915.1

C. Head and Neck Magnet

Another future application of Prepolarized MRI could be head and neck imaging for diagnosing tobacco-related

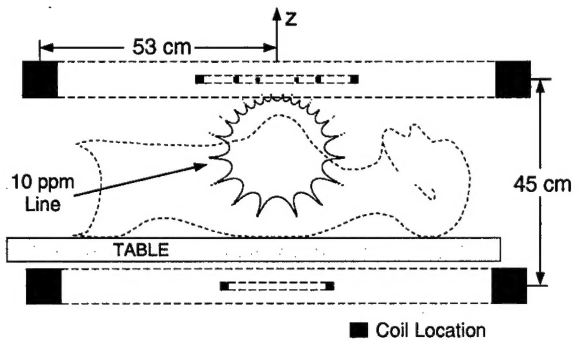

Fig. 6. A biplanar mammography concept magnet designed using the asymmetric geometrical constraints shown in the figure above. The final design had 6 coils, 4 above the homogeneous volume and 2 below. The maximum radius of the coils is 53 cm. We also designed a symmetric magnet with 60-cm gap (not shown) and found that the power increased from 9.8 kW to 15 kW. The simulated field magnitude contour shows the field uniformity constraint was achieved.

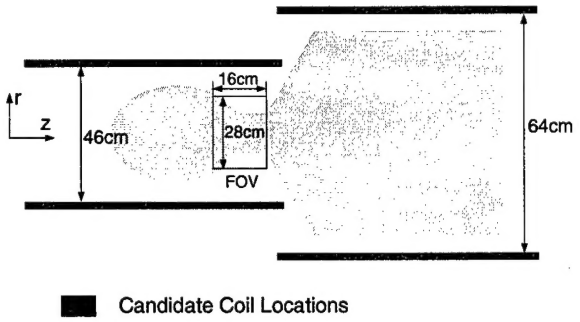

Fig. 7. Candidate coils tailored for a head and neck magnet. The narrower coils with 46 cm diameter are just large enough for the head. The wider coils with 64 cm diameter to allow shoulder access. The homogeneous volume is cylinder shaped to best fit the imaging part.

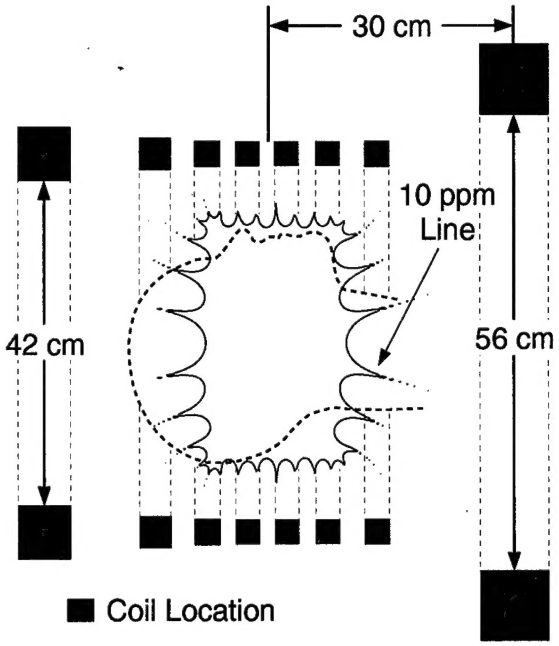

Fig. 8. Head and neck magnet. This is the minimum-power magnet designed with the constraints shown in Fig. 7. This design dissipates 7 kW at 70 mT. An equi-radius magnet with all coils having 56-cm inner diameter would dissipate 10 kW. By using a cylindrically shaped homogeneous volume we can image as close as possible to the shoulders. This design also integrates well with a polarizing coil.

cancer. Here the challenge is to provide a useful imaging volume in the neck and head while minimizing the magnet size to reduce the power. A Garrett-style head-sized magnet is too long for a typical human neck — the homogeneous volume is about 25 cm from the edge of the magnet. An obvious alternative is to make the entire magnet bore large enough (about 60 cm) to admit the shoulders, but this increases the magnet cost. So we pushed the geometric constraints to move the homogeneous homogeneous volume as close as possible to the edge of the magnet. We shaped the feasible coils to just fit the head and shoulders. Instead of a homogeneous sphere, we specified a cylindrical shaped homogeneous volume to just fit the imaging volume. It is 16 cm in thickness, 28 cm in diameter and homogeneous to 10 ppm. The feasible coils and the homogeneous volume are shown in Fig. 7.

As shown in Fig. 8, the head and neck magnet has one coil with a 56 cm inner bore and the remaining coils have 42 cm inner bore, just large enough to fit the head. The 10 ppm lines shown in the figure is the simulated field magnitude. The magnet's specifications are presented in Table III. We calculated the coil size assuming a 408A/cm^2 current density. This magnet consumes 7 kW at 70 mT and it weighs 221 kg. The homogeneous volume is only 5 cm from the right edge of the narrow bore coils, which provides comfortable access to the neck area. A 56-cm-bore equi-radius design would dissipate 10 kW at the same field strength, and would greatly complicate integration with the polarizing magnet.

TABLE III
70 MT HEAD AND NECK MAGNET SPECIFICATIONS.

	r (cm)	z (cm)	I (A)
Coil 1	23.00	-28.26	14984.7
Coil 2	23.00	-14.48	4759.2
Coil 3	23.00	-8.00	2952.9
Coil 4	23.00	-3.00	2584.3
Coil 5	23.00	1.84	2497.7
Coil 6	23.00	6.90	2520.7
Coil 7	23.00	13.00	2799.3
Coil 8	32.00	30.00	26439.1

D. Superconducting Magnet with Active Shielding

We have also found that superconducting magnets can be designed using the ℓ_1-norm minimization method. For superconductors, we would like to minimize the cost of the magnet, which we assume to be proportional to conductor mass. This cost model assumes that the cost of the mechanical reinforcing structure and of the cryostat will not

vary a great deal with the precise coil layout. There may be situations where this is not valid.

The conductor mass is proportional to:

$$\text{Conductor Mass} \propto \sum_{n=1}^{N} 2\pi r_n S_n \,, \tag{13}$$

where r_n and S_n are the radius and cross section respectively for each of the coils. Now $S_n = |i_n|/J$, and we once again assume that the current density, J, is constant. Then the conductor mass is proportional to:

$$\text{Conductor Mass} \propto \frac{2\pi}{J} \sum_{n=1}^{N} r_n |i_n| \,, \tag{14}$$

which is again a radius-weighted ℓ_1-norm of the currents, just like the minimum-power design. This means that resistive and superconducting magnet design problems are equivalent.

In related prior work, Kitamura et al. [13] proposed a minimum-conductor-volume magnet design approach in 1994. Specifically, they minimized the quantity

$$\sum_{n=1}^{N} \frac{S_n j_n}{J_{\max}} \,, \tag{15}$$

where j_n and S_n are the current density and cross-sectional area of the nth coil. To guarantee field homogeneity, they constrained the magnitude of the lower spherical harmonics of the field. They also used linear programming to solve this initial magnet design problem. The results of the linear programming search were then used to initiate a nonlinear optimization algorithm that incorporated the magnetic materials outside the magnet [13]. Their conductor volume expression is similar to ours, but it assumes equi-radius magnets and unidirectional current flow. Our algorithm is appropriate for designing actively shielded MRI magnets, which use bidirectional currents at two or more radii.

Safety considerations in a clinical environment prompt magnet designers to limit the spatial extent of the magnetic field. Magnetic materials are often used to *passively shield*, i.e., to reduce the field outside of the shield. Superconducting magnets are now often designed with so called *active shielding constraints*. Here we design the magnet to satisfy both the homogeneity constraints and the field shielding constraint. The first step in incorporating active shielding is to define the shielding condition — typically this is the desired perimeter for a 5 Gauss line. We then incorporate the shielding constraints into the algorithm by adding distant target field inequality constraints. We also must add extra shield coils to the feasible coil locations; these require a larger diameter than the primary coils. The new shielding constraints at the 5 Gauss line add new inequality constraints to the optimization problem. Specifically, we define two matrices, C_r and C_z, to be the B_z and B_r fields at the shielding locations due to a unit current in the candidate coils. Here we avoid constraining the field magnitude since this represents a nonlinear constraint, which cannot be handled with Linear Programming. Instead we constrain the magnitude of the two field components. Some experimentation was required, and we found that 4.5 Gauss and 3 Gauss were adequate constraints on B_z and B_r at the shielding locations to ensure that the field magnitude was less than 5 Gauss.

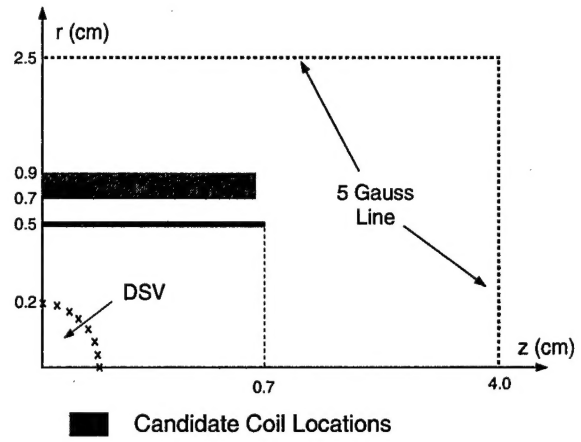

Fig. 9. Active shielding of a superconducting magnet. To design an actively shielded magnet, extra field constraints at the 5 Gauss shielding cylinder are added to the LP problem. Also extra candidate coils at a larger radius are added for the shield.

Hence, the shielding constraints are

$$|C_z\,\mathbf{i}| \;\leq\; B_{z,\text{shield}} \tag{16}$$
$$|C_r\,\mathbf{i}| \;\leq\; B_{r,\text{shield}} \tag{17}$$

For superconducting magnet design with active shielding, we arrive at the following optimization problem.

$$\begin{aligned} \text{Minimize}: \quad & \mathbf{r}^T\mathbf{t} \\ \text{Subject to}: \quad & A\,\mathbf{i} \;\leq\; B_0(1+\epsilon), \\ & -A\,\mathbf{i} \;\leq -B_0(1-\epsilon), \qquad (18) \\ & |C_z\,\mathbf{i}| \;\leq B_{z,\text{shield}} \\ & |C_r\,\mathbf{i}| \;\leq B_{r,\text{shield}} \qquad (19) \\ & |i_n| \;\leq\; t_n, \;\; n = 1 \cdots N. \end{aligned}$$

Fig. 9 shows the feasible coil locations for a symmetric whole body magnet. Here we specified a 1D array of candidate coils at 50 cm radius for the main field and a 2D array of coils extending from 70 cm to 90 cm radius for the shield coils. The maximum z extent of the shield coils was constrained to be slightly smaller than the main field coils to avoid lengthening the design. The specifications were 1 Tesla main field with a 40-cm-DSV and 1 ppm homogeneity. The 5 Gauss line was enforced on a cylinder with 2.5 m radius and 4 m half-length.

Given the feasible coil locations shown above we designed the shielded superconducting magnet shown in Fig. 10. The simulated field magnitude shows that the 5 Gauss line

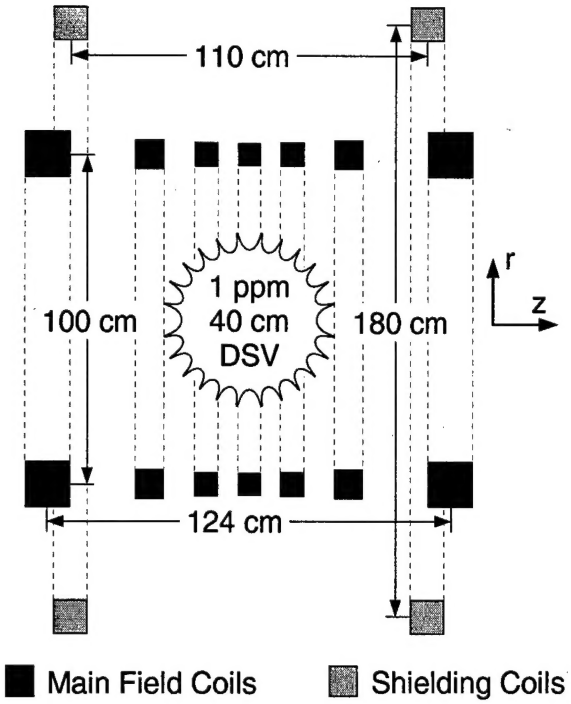

Fig. 10. Shielded magnet design. This actively shielded magnet has 7 primary coils and 2 shielding coils. The current direction is opposite in the two shielding coils. The simulated field magnitude shows the 1 ppm homogeneity contour at the desired 40 cm DSV.

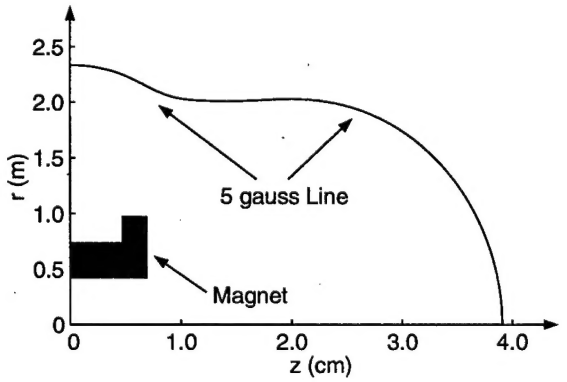

Fig. 11. Simulation of the field magnitude far from the center of the bore. As expected, the 5 gauss line constraint was achieved on the surface of a cylinder with radius 2.5 m and length 4 m.

constraint was achieved, as shown in Fig. 11. The magnet specifications are listed in Table IV. There are seven primary coils and two shielding coils. We assumed that the superconducting current density was J = 4000 A/cm^2.

IV. Summary and Conclusion

We have introduced an algorithm for designing homogeneous resistive and superconducting air-core electromagnets. This new algorithm is fast and flexible enough to handle arbitrarily shaped homogeneous volumes as well as arbitrarily shaped coil formers. Our method assumes a linear relation between the magnetic field and the magnet current. Hence, any magnet that employs high-mu magnetic materials cannot be designed currently using this algorithm. The algorithm is based on the realization that magnet design (either minimum-power or minimum-mass) is equivalent to minimizing the radius-weighted ℓ_1-norm of current. It is fortuitous that ℓ_1-norm problems can be solved very efficiently using standard linear programming modules. Because of the sparseness of the ℓ_1-norm minimization solution, the algorithm automatically chooses the fewest number of coils necessary to meet the design constraints. This key characteristic makes the algorithm practical. Although the algorithm requires no iteration, we prefer to iterate to improve both the coil location precision and also to more accurately model the field due to coils of finite thickness. We demonstrated the flexibility of our new algorithm on three resistive magnet designs and one shielded superconducting magnet design for MRI. Because the algorithm can design a magnet in just a few seconds, it becomes feasible to iteratively design magnets by adjusting the geometric constraints in real-time.

TABLE IV
Magnet specifications for a superconducting 1.0 T shielded magnet.

	r (cm)	z (cm)	I (A)
Coil 1	50.00	0	130974
Coil 2	50.00	± 13.21	154391
Coil 3	50.00	± 30.60	241225
Coil 4	50.00	± 62.08	624542
Coil 5	90.00	± 55.00	-322056

Acknowledgments: We wish to thank Professor Stephen Boyd, whose class on convex optimization introduced us to the theoretical background for this work. We also want to thank Maryam Fazel Sarjoui, and Arash Hassibi for their help with references and suggestions on linear programming packages. Finally we want to thank Zi-Ning Wu for his technical assistance on this project.

The authors gratefully acknowledge the support of research grants from the Whitaker Foundation (176W156), the California Tobacco-Related Disease Research Program (6RT-0384), the ARMY BCRP program (DAMD17-98-1-8157), and the NIH R21 program (R21 HL60328-01).

References

[1] Marcel J. E. Golay, "Field homogenizing coils for nuclear spin resonance instrumentation," *Rev. Sci. Instrum.*, vol. 29, pp. 313, 1958.

[2] J. R. Baker, "An improved three-coil system for producing a uniform magnetic field," *J. Sci. Instrum.*, vol. 27, pp. 197, 1950.

[3] M. W. Garrett, "Calculation of fields, forces and mutual inductances of current system by elliptic integrals," *J. Appl. Phys.*, vol. 34, pp. 2567, 1963.

[4] Milan Wayne Garrett, "Thick cylindrical coil systems for strong magnetic fields with field or gradient homogeneities of the 6th to 20th order," *J. Appl. Phys.*, vol. 38, pp. 2563, 1967.

[5] G. Grossl, F. Winter, and R. Kimmich, "Optimisation of magnet coils for NMR field-cycling experiments," *Journal of Physics E*, vol. 18, pp. 358, 1985.

[6] Herve Saint-Jalmes and Jacques Taquin, "Optimization of homogeneous electromagnetic coil systems: Application to whole-

body NMR imaging magnets," *Rev. Sci. Instrum.*, vol. 52, pp. 1501, 1981.

[7] Katsuji Kaminishi and Shigenori Nawata, "Practical method of improving the uniformity of magnetic fields generated by single and double Helmholtz coils," *Rev. Sci. Instrum.*, vol. 52, pp. 447, 1981.

[8] R. Merritt, C. Purcell, and G. Stroink, "Uniform magnetic field produced by three, four, and five squared coils," *Rev. Sci. Instrum.*, vol. 54, pp. 879, 1983.

[9] H. Siebold, H. Huebner, L. Soelsner, and Th. Reichert, "Performance and results of a computer program for optimizing magnets with iron," *IEEE Trans. Mag.*, vol. 24, pp. 419, 1988.

[10] M. D. Ogle and J. D'Angelo, "Design optimization method for a ferromagnetically self-shield MR magnet," *IEEE Trans. Mag.*, vol. 27, pp. 1689, 1991.

[11] G. Drago, A. Manella, M. Nervi, M. Repetto, and G. Secondo, "A combined strategy for optimization in non-linear magnetic problems using simulated annealing and search techniques," *IEEE Trans. Mag.*, vol. 28, pp. 1541, 1992.

[12] S. Noguchi and A. Ishiyama, "Optimal design method for MRI superconducting magnets with ferromagnetic shield," *IEEE Trans. Mag.*, vol. 33, pp. 1904, 1997.

[13] M. Kitamura, S. Kakukawa, K. Mori, and T. Tominaka, "An optimal design technique for coil configuraions in iron-shielding MRI magnets," *IEEE Trans. Mag.*, vol. 30, pp. 2352, 1994.

[14] M. Souza, C. Vidigal, J. Taquin, and M. Sauzade, "Optimal design of a self shielded magnetic resonance imaging magnet," *Journal De Physique III*, vol. 3, pp. 2121, 1993.

[15] A. K. Kalafala, "A design approach for actively shielded MRI magnets," *IEEE Trans. Mag.*, vol. 26, pp. 181, 1990.

[16] A. K. Kalafala, "Optimized configuration for actively shielded MRI magnets," *IEEE Trans. Mag.*, vol. 27, pp. 1696, 1990.

[17] M. Fujita, "The coil design of the superconducting MRI magnet," *IEEE Trans. Mag.*, vol. 24, pp. 2907, 1988.

[18] A. Ishiyama, K. Shimizu, and A. Sakahara, "An optimal design method for multi-section superconducting magnets using modified simulated annealing," *IEEE Trans. Mag.*, vol. 30, pp. 3435, 1994.

[19] F. J. Davies, R. T. Elliott, and D. G. Hawksworth, "A 2-Tesla active shield magnet for whole body imaging and spectroscopy," *IEEE Trans. Mag.*, vol. 27, pp. 1677, 1991.

[20] D. G. Hawksworth, I. L. McDougall, and J. M. Bird, "Considerations in the design of MRI magnets with reduced stray field," *IEEE Trans. Mag.*, vol. 23, pp. 1309–1314, 1987.

[21] S. Russenschuck, "Synthesis, inverse problems and optimization in computational electromagnetics," *International Journal of Numerical Modelling: Electronic Networks, Devices and Fields*, vol. 9, pp. 45–57, 1996.

[22] Stuart Crozier and David M. Doddrell, "Compact MRI magnet design by stochastic optimization," *J. Magn. Reson.*, vol. 127, pp. 233, 1997.

[23] Stuart Crozier, Lawrence K. Forbes, and David M. Moddrell, "A novel, open access, elliptical cross-section magnet for paediatric MRI," *Meas. Sci. Technol.*, vol. 9, pp. 113, 1998.

[24] Yan Zhang, S. Han, and Z.X. Feng, "The investigation of the superconducting NMR-imaging main magnet," *IEEE Trans. Mag.*, vol. 25, pp. 1881, 1989.

[25] D. A. Lowther, W. Mai, and D. N. Dyck, "A comparison of MRI magnet design using a hopfield network and the optimized material distribution method," *IEEE Trans. Mag.*, vol. 34, pp. 2885, 1998.

[26] L. B. Lugansky, "Optimal coils for producing uniform magnetic fields," *Rev. Sci. Instrum.*, vol. 39, pp. 1372, 1986.

[27] L. B. Lugansky, "On optimal synthesis of magnetic field," *Rev. Sci. Technol.*, vol. 1, pp. 53, 1990.

[28] Sergio Pissanetzky, "Structured coils for NMR applications," *IEEE Trans. Mag.*, vol. 28, pp. 1961, 1992.

[29] Robert Turner, "A target field approach to optimal coil design," *J. Phys. E: Scientific Instruments*, vol. 19, pp. 147–151, 1986.

[30] Michael R. Thompson, Robert W. Brown, and Vishnu C. Srivastava, "An inverse approach to the design of MRI main magnets," *IEEE Trans. Mag.*, vol. 30, pp. 108, 1994.

[31] M. Engelsberg, Ricardo E de Souza, and Carlos M Dias Pazos, "The limitations of a target field approach to coil design," *Journal Of Physics D*, vol. 21, pp. 1062, 1988.

[32] D. I. Hoult and Roxanne Deslauriers, "Accurate shim-coil design and magnetic field profiling by a power-minimization-matrix method," *J. Magn. Reson.*, vol. 108, pp. 9, 1994.

[33] K. H. Schweikert, R. Krieg, and F. Noack, "A high-field air-core magnet coil design for fast-field-cycling NMR," *J. Magn. Reson.*, vol. 78, pp. 77, 1988.

[34] P. Morgan, S. Conolly, and A. Macovski, "Design of uniform field biplanar magnet designs," in *Proceedings of the ISMRM*, May 1997, p. 1477.

[35] Patrick N. Morgan, Steven M. Conolly, and Albert Macovski, "Resistive homogeneous MRI magnet design by matrix subset selection," *Magn. Reson. Med.*, vol. Accepted for Publishing, 1999.

[36] H. Xu, S. Conolly, G.C. Scott, and A. Macovski, "Minimum power homogeneous magnet design for prepolarized MRI," in *39th Experimental NMR Conference*, March 1998, p. 140.

[37] H. Xu, S. Conolly, G.C. Scott, and A. Macovski, "Minimum power homogeneous magnet design for prepolarized MRI," in *Proceedings of the ISMRM*, May 1998, p. 2006.

[38] D. B. Montgomery, *Solenoid Magnet Design*, Krieger, Huntington, 1980.

[39] Philip E. Gill, Walter Murray, and Margaret H. Wright, *Practical Optimization*, Academic Press, London, 1981.

[40] Optimization Technology Center, "Pcx, software for linear programming," http://www.mcs.anl.gov/otc/Tools/PCx, 1998.